Consequences of a unified, anarchical model of fermion masses and mixings

JHEP03(2009)031

(http://iopscience.iop.org/1126-6708/2009/03/031)

JHEP

Published by IOP Publishing for SISSA

Received: *December 15, 2008*
Revised: *January 27, 2009*
Accepted: *February 6, 2009*
Published: *March 5, 2009*

Consequences of a unified, anarchical model of fermion masses and mixings

L. Calibbi, L. Ferretti, A. Romanino and R. Ziegler

SISSA/ISAS,
I–34013 Trieste, Italy
INFN,
I–34013 Trieste, Italy

Abstract: We show that most features of the mass and mixing pattern of the second and third SM fermion families can be accounted for without making use of flavour symmetries or other types of flavour dynamics. We discuss the implications for flavour phenomenology, in particular for the $\tau \to \mu\gamma$ decay rate, and comment on LFV effects at colliders. We show that the model can be embedded in a full SO(10) supersymmetric GUT in 5 dimensions that preserves the successful MSSM gauge coupling unification prediction for α_s. Interesting features of this embedding are i) the connection of one of the hierarchy parameters with the strong coupling assumption, ii) the absence of KK threshold effects on the α_s prediction at one loop, and iii) the shift of the GUT scale up to about 10^{17} GeV. Proton decay is under control, also due to the larger GUT scale. A large atmospheric angle for normal hierarchical neutrinos is obtained in an unusual way.

Keywords: Rare Decays, Beyond Standard Model, Quark Masses and SM Parameters, GUT

ArXiv ePrint: 0812.0087

doi:10.1088/1126-6708/2009/03/031

JHEP03(2009)031

Contents

JHEP03(2009)031

1 Introduction

Different approaches have been used so far to explain the peculiar pattern of fermion masses and mixings and in particular to account for the widely different patterns observed in the charged and neutral fermion sectors.

While the experimental determination of neutrino masses and mixings is relatively recent, the first charged fermion mass was measured more than a century ago. As a consequence, most approaches, most notably the one based on flavour symmetries, have been developed in connection to the charged fermion sector and have been later extended to neutrinos and lepton mixing. This is also because charged fermion masses may be related to the origin of flavour in a more direct way than neutrinos, as the latter are likely to get their masses from lepton number violation at large scales through some kind of see-saw mechanism.

Following [1], in this paper we will consider an "anarchical" approach that does not make use of any flavour symmetry [2] or other dynamical mechanisms and can be considered to be inspired by the neutrino sector. It is well known that the structure of masses and

mixings of the second and third neutrino families can be accounted for in terms of the dominant exchange of a single right-handed neutrino with similar, possibly large couplings to both the second and third light neutrinos [3]. This leads to a normal-hierarchical pattern of light neutrinos. As the couplings can be taken to be random order one numbers, this mechanism does not require any special dynamics controlling the sizes of the couplings of the second and third families. Still, the neutrino spectrum ends up being hierarchical, for the simple reason that the exchange of a single singlet neutrino can only give mass to one light neutrino.

Is it possible that a similar mechanism is at work in the charged fermion sector, with the structure of masses and mixings of the second and third charged fermion families accounted for by the dominant exchange of a single set of messengers, with unconstrained, anarchical, $\mathcal{O}(1)$ couplings? On the one hand, the single messenger mechanism can in principle be exported, since many theories of flavour, including those based on flavour symmetries, assume the existence of a heavy sector of messengers. On the other hand, the extension to the quark sector might look non-trivial, since the random $\mathcal{O}(1)$ couplings lead in the neutrino sector to large mixing angles that we do not observe in the quark sector. This potential problem, however, does not arise if the messengers are left-handed, as observed in [1]. In this case, in fact, the large rotations induced in the up and down quark sector are approximately equal and compensate each other, leading to small mixing in the CKM matrix. Starting from this observation, a Pati-Salam (PS) model was developed that accounts for most features of the masses and mixings of the second and third families and for the main qualitative features associated with the first family. While some specific flavour dynamics may need to be invoked for a quantitative account of the first family, it is impressive that so many other features do not actually need a flavour symmetry or other dynamics to be explained.

In this paper, we show that the approach illustrated in [1] can be embedded in a unified theory, more precisely in a SO(10) supersymmetric model in five dimensions. We also discuss the implications for flavour changing neutral current (FCNC) and lepton flavour violating (LFV) processes. We begin in section 2 illustrating the pattern of fermion masses and mixings emerging from the unified theory in the context of a simple, effective PS theory in four dimensions. In section 3 we illustrate the peculiar FCNC and LFV effects associated with new physics near the GUT scale characterized by large couplings with both the second and third family. In section 4 we show an example of embedding in SO(10). In most of the paper we concentrate on the second and third family masses and mixings, whose features do not need flavour symmetries. In section 4.7, before concluding, we sketch a possibility to fix the quantitative aspects related to the first family. For sake of clarity, we will give a short summary of the basic assumptions and achievements at the end of each section.

2 Yukawa textures in the effective Pati-Salam theory

We begin by illustrating the model at scales lower than the compactification scale at which the unified structure emerges. As we will see in section 4, SO(10) is broken at those scales to the Pati-Salam (PS) gauge group $G_{\rm PS} = {\rm SU}(2)_L \times {\rm SU}(2)_R \times {\rm SU}(4)_c$ and inherits

JHEP03(2009)031

	f_i	f_i^c	h	ϕ	F	$\bar{F}$	F^c	$\bar{F}^c$	F'_c	$\bar{F}'_c$	X_c	Σ
$\mathrm{SU}(2)_L$	2	1	2	1	2	2	1	1	1	1	1	1
$\mathrm{SU}(2)_R$	1	2	2	1	1	1	2	2	2	2	3	1
$\mathrm{SU}(4)_c$	4	$\bar{4}$	1	15	4	$\bar{4}$	$\bar{4}$	4	$\bar{4}$	4	1	15
$\mathbf{Z}_2$	$-$	$-$	$-$	$-$	$+$	$+$	$+$	$+$	$+$	$+$	$+$	$+$
R_P	$-$	$-$	$+$	$+$	$-$	$-$	$-$	$-$	$+$	$+$	$+$	$-$

Table 1. Chiral field content and quantum numbers under G_{PS} and $\mathbf{Z}_2$

two discrete symmetries, a parity $\mathbf{Z}_2$ and an R-parity R_P, from the full unified model. The chiral superfield content and the corresponding quantum numbers under the gauge and discrete symmetries are summarized in table 1. The first block contains the $\mathbf{Z}_2$-odd fields: the 3 light (in the unbroken $\mathbf{Z}_2$ limit) families (f_i, f_i^c), $i = 1, 2, 3$, the light Higgs h, and the $\mathbf{Z}_2$-breaking field ϕ. The latter is assumed to be in the adjoint representation of $\mathrm{SU}(4)_c$ as this provides the Georgi-Jarlskog factor 3 needed to account for the μ–s mass relation. The second block contains the messengers, in a single vectorlike family $(F, F_c)+(\bar{F}, \bar{F}_c)$. The third block contains the fields $F'_c+\bar{F}'_c$ and X_c providing the necessary breaking of the Pati-Salam group. Finally, the field Σ in the last column is needed to communicate the $\mathrm{SU}(2)_R$ breaking provided by $F'_c + \bar{F}'_c$ to the messengers $F_c + \bar{F}_c$. The up and down components of those messengers need in fact to be different in order to account for $m_c/m_t \ll m_s/m_b$. The field content is thus rather economical. We will later add another few PS fields in order to preserve gauge coupling unification above M_R and to take care of singlet neutrino masses. As we will see, the MSSM 1-loop gauge unification turns out to be exactly preserved. The decomposition of the fields in table 1 under the SM gauge group is the following (with hopefully self-explanatory notations): $F = (L, Q)$, $\bar{F} = (\bar{L}, \bar{Q})$, $F^c = (L^c, Q^c)$, $\bar{F}^c = (\bar{L}^c, \bar{Q}^c)$, $L^c = (N^c, E^c)$, $Q^c = (U^c, D^c)$, $\bar{L}^c = (\bar{N}^c, \bar{E}^c)$, $\bar{Q}^c = (\bar{U}^c, \bar{D}^c)$, $\phi = (A_\phi, T_\phi, \bar{T}_\phi, G_\phi)$, where A_ϕ is a singlet, $T_\phi \sim (3, 1, 2/3)$, $\bar{T}_\phi \sim (\bar{3}, 1, -2/3)$, $G_\phi \sim (8, 1, 0)$ under $\mathrm{SU}(3)_c \times \mathrm{SU}(2)_L \times \mathrm{U}(1)_Y$ (all fields are properly normalized). Analogously for the other fields with the same quantum numbers under PS. We also denote $a \langle X_c \rangle = M_R \sigma_3$, $\langle N'_c \rangle = V_c$, $\langle \bar{N}'_c \rangle = \bar{V}_c$ ($|V_c| = |\bar{V}_c|$ in the supersymmetric limit), $\langle \phi \rangle = M_L T_{B-L}$.

At this effective level, the model is characterized by two scales, M_R and M_L, with $M_R > M_L$, corresponding to the masses of the right-handed and left-handed messengers. The PS group is spontaneously broken to the SM group at the scale M_R. Up to some explicit mass terms, whose absence will be accounted for by the full theory in section 4, the most general renormalizable superpotential for the fields in table 1 is

$$W = \lambda_i f_i^c F h + \lambda_i^c f_i F^c h + \alpha_i \phi f_i \bar{F} + \alpha_i^c \phi f_i^c \bar{F}^c + a \bar{F}^c X_c F^c + \bar{\sigma}_c \bar{F}'_c \Sigma F^c + \sigma_c \bar{F}^c \Sigma F'_c + \frac{M_\Sigma}{2} \Sigma^2 \ldots . \tag{2.1}$$

All the couplings are assumed to be $\mathcal{O}(1)$ and uncorrelated. The terms involving R_P-even fields only, providing the vevs of the fields F'_c, $\bar{F}'_c$, X_c, ϕ along the SM invariant directions, have been omitted, as they do not affect fermion masses directly. They will be discussed in section 4. The $\mathbf{Z}_2$ conserving vevs lie near a single scale, M_R, the scale of the right-

handed messengers F^c, $\bar{F}^c$. The $\mathbf{Z}_2$-breaking vev of ϕ lies at the smaller scale M_L, the scale of the left-handed messengers F, $\bar{F}$. The hierarchy of SM fermion masses originates from $\epsilon \equiv M_L/M_R \ll 1$. This means that the hierarchy among different family masses originates from a hierarchy within a single family of messengers (which in turn is related to the hierarchy between two PS-breaking vevs).

Non renormalizable terms in the superpotential involving vevs at the scale M_R could give rise (or not) to mass terms comparable with the scale M_L. Such mass terms could be relevant for the left-handed messengers F, $\bar{F}$, which do not get a mass at the scale M_R. In the context of the full model, such a mass term does not arise.[1] We assume that the Higgs field h remains massless. This will be also accounted for in the full model, in terms of an R-symmetry.

In order to identify the light (massless in the unbroken EW symmetry limit) MSSM fields, we plug the vevs in the superpotential in eq. (2.1). Since R_P is not broken at this level, the R_P-even and R_P-odd heavy fields do not mix, and we can restrict our analysis to the R_P-odd fields. We choose a basis in flavour space such that $\lambda_{1,2} = \alpha_{1,2} = 0$, $\lambda_1^c = \alpha_1^c = 0$. λ_3, α_3, $\lambda_{2,3}^c$, $\alpha_{2,3}^c$, M_R, v, $V_c = \bar{V}_c$ can all be taken positive. The heavy mass terms turn out to be

$$- \bar{E}^c \left[M_R E^c - M_L \left(\alpha_3^c e_3^c + \alpha_2^c e_2^c\right)\right] - \alpha_3 M_L \bar{L} l_3 \tag{2.3}$$

$$- \bar{D}^c \left[M_R D^c + \frac{M_L}{3}\left(\alpha_3^c d_3^c + \alpha_2^c d_2^c\right)\right] + \alpha_3 \frac{M_L}{3} \bar{Q} q_3 \tag{2.4}$$

$$+ \bar{U}^c \left[M_R U^c - \frac{\sigma_c}{\sqrt{2}} V_c \bar{T}_\Sigma - \frac{M_L}{3}\left(\alpha_3^c u_3^c + \alpha_2^c u_2^c\right)\right] + T_\Sigma \left[M_\Sigma \bar{T}_\Sigma - \frac{\bar{\sigma}_c}{\sqrt{2}} \bar{V}_c U^c\right] + \frac{M_\Sigma}{2} G_\Sigma^2 \tag{2.5}$$

$$+ \bar{N}^c \left[M_R N_c + M_L \left(\alpha_3^c n_3^c + \alpha_2^c n_2^c\right)\right] + \sqrt{\frac{3}{8}} \sigma_c V_c \bar{N}^c A_\Sigma + \sqrt{\frac{3}{8}} \bar{\sigma}_c \bar{V}_c N^c A_\Sigma + \frac{M_\Sigma}{2} A_\Sigma^2. \tag{2.6}$$

Because of the absence of $\bar{L}L$ and $\bar{Q}Q$ mass terms, L and Q remain massless, while l_3 and q_3 get a mass together with $\bar{L}$ and $\bar{Q}$ from the vev of ϕ. The light lepton and quark doublets are therefore $l_3' = L$, $l_{1,2}' = l_{1,2}$, $q_3' = Q$, $q_{1,2}' = q_{1,2}$ and the heavy ones are $L' = l_3$, $Q' = q_3$, $\bar{L}' = \bar{L}$, $\bar{Q}' = \bar{Q}$. The light $\mathrm{SU}(2)_L$ singlets can be easily determined along the lines of [1]. The $\mathbf{Z}_2$-even fields D^c, U^c, E^c all contain a small, $\mathcal{O}(\epsilon)$ light component, except U^c, whose light component $u_2^{c\prime}$ can be further suppressed because of the mixing with the color triplets T_Σ, $\bar{T}_\Sigma$ in Σ. A double ϵ suppression is obtained if

$$\frac{M_\Sigma M_R^2}{M_L V_c^2} = \mathcal{O}(1). \tag{2.7}$$

This double suppression then explains why $m_c/m_t \ll m_s/m_b$ [1]. The implementation in section 4 will indeed give $M_\Sigma \sim M_R \sim \sqrt{\epsilon} V_c$.[2]

The light fermion Yukawa matrices Y^D, Y^E, Y^U (in right-left convention) are easily determined expressing the superpotential in terms of the massless fields. At the leading

[1] This represents a difference with respect to [1], where such a mass term was assumed to be present and to be along the $B - L$ direction.

[2] In [1] it was instead assumed that $V_c \sim M_R$ and $M_\Sigma \sim M_L$.

JHEP03(2009)031

order in ϵ we find

$$Y^D = \begin{pmatrix} 0 & 0 & 0 \\ 0 & -\alpha_2^c \lambda_2^c \epsilon/3 & 0 \\ 0 & -\alpha_3^c \lambda_2^c \epsilon/3 & \lambda_3 \end{pmatrix}, \quad Y^E = \begin{pmatrix} 0 & 0 & 0 \\ 0 & \alpha_2^c \lambda_2^c \epsilon & 0 \\ 0 & \alpha_3^c \lambda_2^c \epsilon & \lambda_3 \end{pmatrix},$$
$$Y^U = \begin{pmatrix} 0 & 0 & 0 \\ 0 & -(2/3)\alpha_2^c \lambda_2^c \rho_u \epsilon^2 & 0 \\ 0 & -(2/3)\alpha_3^c \lambda_2^c \rho_u \epsilon^2 & \lambda_3 \end{pmatrix}, \tag{2.8}$$

where $\rho_u = (\sigma_c \bar{\sigma}_c)^{-1} (M_\Sigma M_R^2)/(M_L V_c^2)$ is an order one coefficient. The numerical value of ϵ turns out to be $\epsilon \approx 0.06\, \lambda_3/(\alpha_2^c \lambda_2^c)$, which implies $\rho_u \approx 1.9\, (\alpha_2^c \lambda_2^c/\lambda_3)$, indeed of order one.

The model predicts the first family to be massless in the limit in which non-renormalizable corrections to W are neglected and to be further suppressed by powers of the cutoff once those corrections are taken into account. Unlike the second and third families, the quantitative aspects related to the first family masses may need to be controlled by some flavour dynamics. An example is given in section 4.7.

Neutrino masses will be discussed in the context of the full model in section 4.4.

To summarize, we illustrated a supersymmetric Pati-Salam model aiming at explaining the fermion masses and mixings for the 2nd and 3rd family. This model arises as the low-energy limit of a fully unified model in 5 dimensions, which will be presented in section 4. The low energy effective limit of the full model is useful because it is simple, it contains most of the features relevant for the phenomenology, and it does not depend on the detailed implementation of the full unified model. The full model will also justify most of the assumptions made in this section, which are:

- Besides the Pati-Salam gauge symmetry there are 2 discrete symmetries, $\mathbf{Z}_2$ and R_P.
- All the allowed dimensionless couplings are present and are $\mathcal{O}(1)$; the structure and the scales of the mass terms will be accounted for by the full model in terms of an R-symmetry and a discrete Z_{24}.
- Only the R_P-even fields get a vev (the corresponding dynamics will be specified in the full model).
- We have 4 mass scales M_R, M_L, M_Σ, V_c satisfying the relations

$$M_R \gg M_L, \quad \frac{M_\Sigma M_R^2}{M_L V_c^2} = \mathcal{O}(1),$$

  which account for the mass hierarchy in the down-quark and charged lepton sector and the up-quark sector respectively (these scales will be dynamically justified in the full model).

JHEP03(2009)031

3 FCNC and LFV

In this section we discuss the implications of the effective model discussed in the previous section for Flavour Changing Neutral Current (FCNC) and Lepton Flavour Violation (LFV) effects. Most of the conclusions are independent of the details of the full unified implementation of the model and extend to the model in section 4.

In order to identify the peculiar effects associated to the basic ingredients of the model, we assume the supersymmetric soft terms to be universal at a scale $M_c > M_R$. More precisely, we assume a common value for the gaugino masses, $M_{1/2}$, for the sfermion masses, m_0^2, and for the trilinear terms, A_0, at that scale. As for the Higgs soft masses, we consider the possibility that they are independent, with an average value $(m_h^0)^2 = (m_{H_D}^2 + m_{H_U}^2)/2 = m_0^2$ and a splitting $4m_X^2 = m_{H_D}^2 - m_{H_U}^2$. This is because their splitting m_X^2 can play an important role when $\tan\beta$ is large[3] [4] and because the connection of Higgs and sfermion masses may not be straightforward [6, 7]. For definiteness, we will always take $A_0 = 0$. Motivated by the unified model of section 4, we take M_c as determined by the unification condition ($M_c \sim 10^{16}\,\mathrm{GeV}$ in the region of parameter space in which threshold effects are favourable) and we also consider the limit $m_0^2 = m_X^2 = 0$ in which the only sizable high-energy parameter is the common gaugino mass and the low-energy scalar soft masses and trilinear terms are generated by the RGE running.

3.1 The pattern of the RGE effects

The interactions of MSSM fields at energy much higher than the electroweak scale leave their imprint on the sfermion soft masses through radiative effects. Well known examples are the lepton flavour violating effects induced by see-saw [8] and GUT [9] interactions. In the model described in the previous section, the MSSM fields interact with the left-handed and right-handed flavour-messengers living at the scales M_L and M_R respectively. The peculiar feature of our model is that the corresponding Yukawa interactions (with all the three light families) are described by $\mathcal{O}(1)$ couplings, not constrained to be small by any symmetry. We therefore expect the flavour-violating effects induced in the sfermion mass matrices to be sizable.

In order to get an analytical understanding of the effects, we write the off-diagonal sfermion mass terms induced by the extra-interactions at M_L and M_R in the leading logarithm approximation. Also, we use the same basis in flavour space that leads to the textures in eq. (2.8). The flavour-violating effects turn out to be quite different for right- and left-handed sfermions. Let us start with the right-handed ones. The light eigenstates turn out to be in the form $f_i'^c = f_i^c - \epsilon\,\alpha_i^c (B-L) F^c$, with $\epsilon \sim 0.06$ and $i = 1,2,3$. Therefore, their soft mass matrix is given, in first approximation, by the soft mass matrix $\tilde{m}_{f^c}^2$ for the three

[3] In this regime $\lambda_t \approx \lambda_b \sim O(1)$ and the RGEs for $m_{H_D}^2$ and $m_{H_U}^2$ are similar. If $m_{H_D}^2 = m_{H_U}^2$ to start with, it is difficult to have at the same time $m_{H_U}^2 + \mu^2$ negative enough to break the electroweak gauge symmetry and $m_{H_D}^2 + \mu^2$ positive enough so that the squared pseudoscalar Higgs mass is positive. The splitting m_X between the two Higgs soft terms can be given by additional contributions to the soft SUSY breaking scalar masses arising from the D-terms associated with the broken diagonal generators. These contributions are generated whenever the soft SUSY-breaking masses of the fields whose vacuum expectation values reduce the rank of the group are different [5].

JHEP03(2009)031

fields f_i^c. eq. (2.1) shows that the latter have two sizable flavour-dependent interactions, the one with the left-handed messengers, $\lambda_i f_i^c F h$, and the one with the right-handed ones, $\alpha_i^c \phi f_i^c \bar{F}^c$. In the leading logarithm approximation, the right-handed sfermion mass matrix is given by

$$(\tilde{m}^2_{f^c})_{ij} = m_0^2 \delta_{ij} + \frac{1}{(4\pi)^2}\left[\left(21 g^2 M_{1/2}^2 \delta_{ij} - 12 \lambda_i \lambda_j m_0^2\right) \log\frac{M_c}{M_L} - \frac{45}{4}\alpha_i^c \alpha_j^c m_0^2 \log\frac{M_c}{M_R}\right] \quad (3.1)$$

at the scale M_L (below that the running is the same as in the MSSM).

In the basis of eq. (2.8), in which the fermions are almost diagonal, we have $\lambda_1 = \lambda_2 = 0$, so that the left-handed messengers split the third sfermion mass from the first two but do not induce off-diagonal terms. On the other hand, we expect $\alpha_2^c \sim \alpha_3^c \neq 0$, so that the interaction with right-handed messengers will give sizable off-diagonal "2-3" terms. Numerically, we expect $\delta^c_{23} = (\tilde{m}^2_{f_c})_{23}/m_0^2 = \mathcal{O}\left(10^{-1}\right)$.

Things are different for the left-handed sfermions. The light eigenstates are essentially $f_3' = F$, $f_{1,2}' = f_{1,2}$. Therefore, mixed 2-3 terms cannot be generated above the Z_2 breaking scale M_L. Hence, we expect the off-diagonal "2-3" element of the left-handed sfermion mass matrices to be smaller than in the case of right-handed sfermions. A non-negligible value can be generated through the non-universal A-terms, in turn generated (at the next to leading logarithm level) by the running.

The large high-scale Yukawa couplings also have an important effect on the diagonal terms of the scalar masses: both the second and the third family masses receive significant contributions. The third family mass would be anyway split by the MSSM running as an effect of the large third family Yukawas. The splitting of the first two families is instead more peculiar and might induce potentially large FCNC and LFV effects in the "1-2" sector, once the fermion mass matrices are diagonalized in order to go to the so-called SCKM basis. As a consequence, the pattern of the Yukawa entries involving the first family turns out to be constrained, as we will discuss in section 4.7. Summarizing, in the basis leading to eq. (2.8), the slepton soft masses at M_L are in the form

$$m^2_{RR} = \begin{pmatrix} (m^2_{\tilde{e}^c})_{11} & 0 & 0 \\ 0 & (m^2_{\tilde{e}^c})_{22} & (m^2_{\tilde{e}^c})_{23} \\ 0 & (m^2_{\tilde{e}^c})_{23} & (m^2_{\tilde{e}^c})_{33} \end{pmatrix}, \quad m^2_{LL} = \begin{pmatrix} (m^2_{\tilde{l}})_{11} & 0 & 0 \\ 0 & (m^2_{\tilde{l}})_{22} & 0 \\ 0 & 0 & m^2_{\tilde{L}} \end{pmatrix}. \quad (3.2)$$

The running between M_c and M_L gives $(m^2_{\tilde{e}^c})_{11} > (m^2_{\tilde{e}^c})_{22} > (m^2_{\tilde{e}^c})_{33}$ and $(m^2_{\tilde{l}})_{11} > (m^2_{\tilde{l}})_{22} > m^2_{\tilde{L}}$. The full 1-loop RGEs can be found in the appendix.

3.2 Numerical analysis

Exact expressions have been used to compute the branching ratios of LFV decays, $\mathrm{BR}(l_i \to l_j\,\gamma)$ [10], and the SUSY contribution to the anomalous magnetic moment of the muon, $a_\mu = (g-2)_\mu/2$ [11]. The SUSY contributions to $B_{d,s} \to \mu\mu$ are estimated by using the formulas in [12]. The branching ratio $\mathrm{BR}(b \to s\,\gamma)$ is computed using the routine `SusyBSG` [13]. The meson mass splittings (Δm_K, Δm_D, Δm_B, Δm_{B_s}) are used to constrain the SUSY parameter space. The FCNC processes we have studied and the corresponding experimental measurements or bounds are summarized in table 2.

JHEP03(2009)031

Observable	Bound	ref.
$\mathrm{BR}(\mu \to e\gamma)$	$< 1.2 \times 10^{-11}$	[14]
$\mathrm{BR}(\tau \to \mu\gamma)$	$< 6.8 \times 10^{-8}$	[15]
$\mathrm{BR}(\tau \to e\gamma)$	$< 1.1 \times 10^{-7}$	[16]
$\mathrm{BR}(b \to s\gamma)$	$2.77 \times 10^{-4} - 4.33 \times 10^{-4}$ (3σ)	[17]
$\mathrm{BR}(B_s \to \mu\mu)$	$< 4.7 \times 10^{-8}$	[18]
$(\Delta m_{B_s})^{\mathrm{susy}}$	$< 4.6\ \mathrm{ps}^{-1}$ (2σ)	[19]
$\delta a_\mu^{\mathrm{susy}}$	$126 \times 10^{-11} - 478 \times 10^{-11}$ (2σ)	[20]

Table 2. Experimental bounds used in the numerical analysis.

The numerical analysis has been performed by solving the full 1-loop RGEs of the model from the universality scale M_c to M_L and the MSSM RGEs from M_L to $M_{\mathrm{susy}} \equiv \sqrt{m_{\tilde{t}_1} m_{\tilde{t}_2}}$. The high-scale Yukawas are fixed by requiring a good fit of fermion masses and mixings at M_Z. The high-energy parameters which cannot be unambiguously set by low-energy data are chosen to be 1. After the running, the soft mass matrices and A-terms are rotated to the SCKM basis, in which the spectrum and the flavour observables are computed. For each point of the SUSY parameter space, we check that the electroweak symmetry breaking does take place and no tachyonic particles arise. Moreover, to be conservative, we require that the Lightest Supersymmetric Particle (LSP) is the lightest neutralino. Limits on the Higgs and SUSY particles masses from the direct searches at LEP are also imposed.

We consider two different regimes:

- Large $\tan\beta$, as determined by top-bottom unification at M_R. This is the prediction of the minimal model in section 2. We take $m_X = 700\,\mathrm{GeV}$ in this case (see discussion above).

- A lower value of $\tan\beta$, which can be easily obtained in the presence of a mixing in the Higgs sector. We will present the results for the case $\tan\beta = 40$, $m_X = 0$.

In figure 1 we present the prediction for $\mathrm{BR}(\tau \to \mu\,\gamma)$ in the $(m_0,\, M_{1/2})$ plane in the first case. The parameter space is constrained by the requirement of a neutral LSP, by the LEP bound on the Higgs mass, and by $\mathrm{BR}(B_s \to \mu\mu)$. The latter bound has a significant dependence on the value of m_X. In the small m_X limit, in fact, a light CP-odd Higgs enhances the Higgs-mediated contribution[4] to $\mathrm{BR}(B_s \to \mu\mu)$, especially in the large m_0, moderate $M_{1/2}$ region. Larger values of m_X increase m_A, thus alleviating the bound from $B_s \to \mu\mu$.

The present limit $\mathrm{BR}(\tau \to \mu\,\gamma) \lesssim 6.8 \cdot 10^{-8}$ only gives a weak constraint on the parameter space, $(m_0,\, M_{1/2}) \lesssim 1$ TeV. A Super B-Factory able to reach a sensitivity of 10^{-9} [21] would test a large portion of the parameter space shown. The black line in figure 1 corresponds to $\delta a_\mu^{\mathrm{susy}} = 126 \cdot 10^{-11}$. In the region below the black line, the supersymmetric

[4] See [12] and references therein.

JHEP03(2009)031

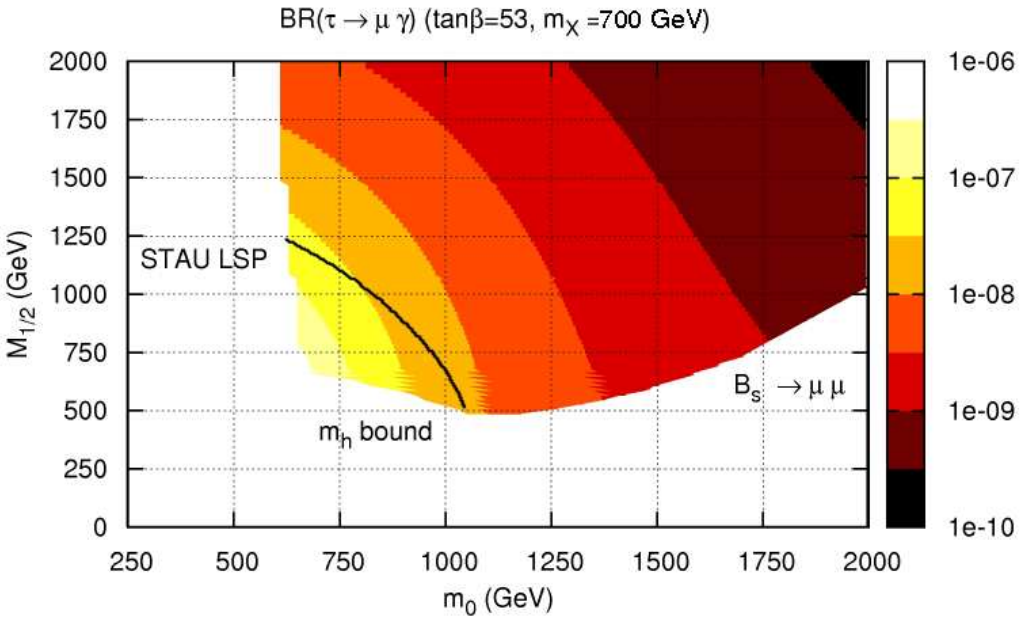

Figure 1. Result for BR($\tau \to \mu\,\gamma$) in the (m_0, $M_{1/2}$) plane for $\tan\beta \approx 53$, as determined by top-bottom Yukawa unification, $m_h^0 = m_0$ and $m_X = 700$ GeV. The black line corresponds to a SUSY contribution to $\delta a_\mu^{\rm susy} = 126 \cdot 10^{-11}$.

contribution to the muon magnetic moment would reduce the present tension [20] between the experimental measurement of the muon magnetic moment and the SM prediction below the 2σ level.

In figure 2 we show contour plots of the lightest stop and gluino masses, for the same choice of the parameters in figure 1. Comparing figure 2 with figure 1, we see that, for the case considered here, a Super B-factory bound BR($\tau \to \mu\,\gamma$) $\lesssim 10^{-9}$ would be able to test almost completely the parameter space for SUSY masses within the LHC reach.

In figure 3 the results for the $\tan\beta = 40$, $m_X = 0$ case are shown for $m_h^0 = m_0$. In this case the parameter space is much less constrained. The low $M_{1/2}$ region is excluded by LEP direct searches for SUSY particles, while $b \to s\,\gamma$ and $B_s \to \mu\mu$ constrain the low m_0, low $M_{1/2}$ regime. The present limit on BR($\tau \to \mu\,\gamma$) does not give rise to additional constraints and the Super B-factory sensitivity should test the parameter space up to (m_0, $M_{1/2}$) $\sim 1\,$TeV. The $(g-2)_\mu$ result favours in this case a region almost completely within the reach of the Super B-factory.

As previously mentioned, some of the high-energy Yukawas are not determined by the fit of the fermion masses and mixings and have been fixed to $\mathcal{O}(1)$ values. In order to show the impact of those $\mathcal{O}(1)$ parameters on BR($\tau \to \mu\,\gamma$), we display in figure 4 a scatter plot where all the unknown Yukawas are independently varied between 0.5 and 1.5. We consider in this case "gaugino-mediation" boundary conditions with $m_0 = m_X = 0$. The figure shows that the $\mathcal{O}(1)$ parameters can conspire to enhance BR($\tau \to \mu\,\gamma$) by up to one order of magnitude.

JHEP03(2009)031

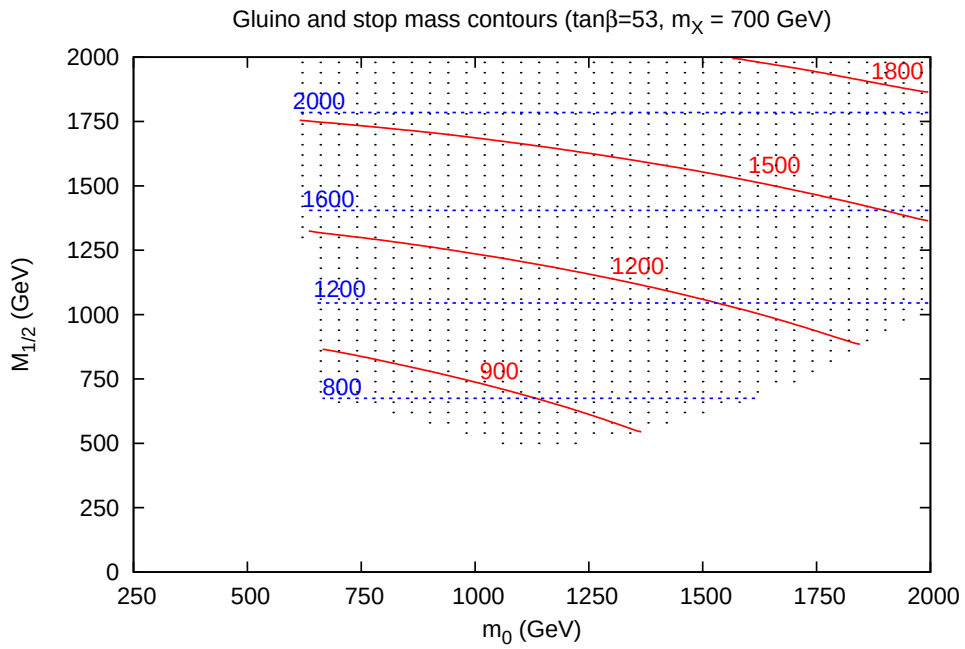

Figure 2. Contour plot for the gluino (blue, dashed lines) and the lightest stop (red, solid lines) ma

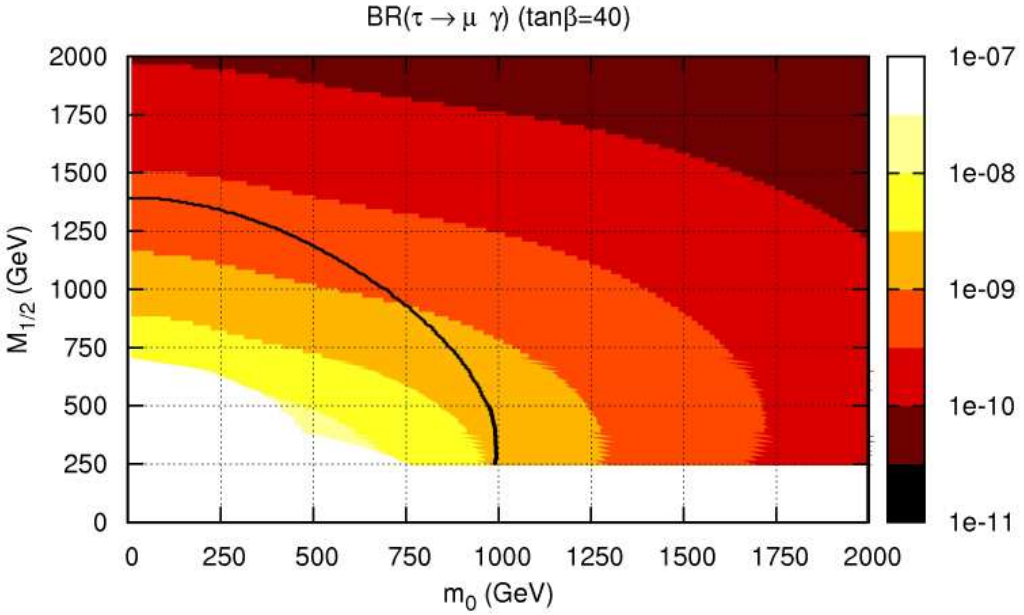

Figure 3. Same as figure 1 for the case with $\tan\beta = 40$, $m_h^0 = m_0$ and $m_X = 0$.

The WMAP constrain on the dark matter relic density [22] can also be accounted for by a neutralino thermal relic within this model. Two examples of parameter space

JHEP03(2009)031

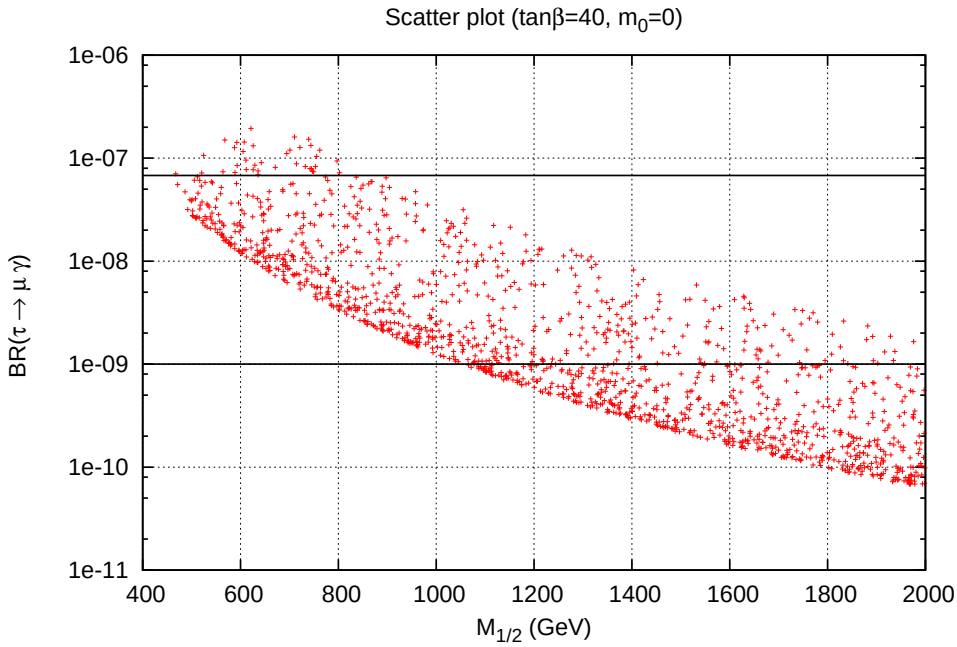

Figure 4. BR($\tau \to \mu\,\gamma$) vs $M_{1/2}$ for $\tan\beta = 40$ and "gaugino-mediation"-inspired boundary conditions ($m_0 = m_h^0 = m_X = 0$). The unknown $\mathcal{O}(1)$ couplings are randomly varied between 0.5 and 1.5. Horizontal lines represent the present bound (6.8×10^{-8}) and the future limit (10^{-9}) on BR($\tau \to \mu\,\gamma$).

Point	$\tan\beta$	m_0	m_h^0	m_X	$M_{1/2}$
A	53	650	650	700	1400
B	40	0	0	0	850

Table 3. Two points of the parameter space accounting for the dark matter relic density. The masses are expressed in GeV.

points leading to the correct density are exhibited in table 3. Point **A** is an example of the unified top-bottom Yukawa regime, point **B** is an example of the $\tan\beta = 40$ case, with gaugino-mediation boundary conditions. For point **A**, the WMAP bound on cold dark matter is satisfied by stau-neutralino co-annihilation [23]. In the case of point **B** the correct relic density is given by the LSP annihilation through the CP-odd Higgs s-channel exchange [24]. In table 4 we show the corresponding SUSY and Higgs spectrum, the predictions for the $b \to s\,\gamma$ branching ratio, the SUSY contribution to the magnetic moment of the muon $\delta a_\mu^{\rm susy}$, $\tau \to \mu\,\gamma$ branching ratio and the DM relic density $\Omega_{\rm DM}\,h^2$, which has been computed using the routine `micrOMEGAs` [25]. For both points LHC should observe several SUSY particles, even if the spectrum of point **A** is heavier. Both points give a BR($\tau \to \mu\,\gamma$) within the sensitivity of the proposed Super B-factory, while point **B** gives a better agreement with $(g-2)_\mu$.

JHEP03(2009)031

	$m_{\tilde{t}_1}$	$m_{\tilde{g}}$	$m_{\tilde{\tau}_1}$	$m_{\tilde{\chi}_1^0}$	m_h	m_A	$\mathrm{BR}(b \to s\,\gamma)$	$\delta a_\mu^{\mathrm{susy}}$	$\mathrm{BR}(\tau \to \mu\,\gamma)$	$\Omega_{\mathrm{DM}}\,h^2$
A	1291	1661	360	339	119	1000	3.15×10^{-3}	105×10^{-11}	2.4×10^{-8}	0.095
B	723	1023	243	202	117	353	3.16×10^{-3}	316×10^{-11}	4×10^{-9}	0.106

Table 4. Spectrum and predictions for the two parameter space points in table 3. The masses are expressed in GeV.

Finally, let us comment on possible LFV effects at the LHC. In the moderate $\tan\beta$ case, the structure of the radiative contributions in eq. (3.1) is particularly interesting in this respect: $\tilde{m}_{ij}^2 = m_0^2\delta_{ij} + \sigma c_{ij} m_0^2$, where c_{ij} is a matrix with $\mathcal{O}(1)$ entries and σ accounts for all the rest, including the loop factors (in the large $\tan\beta$ case, the bottom Yukawa radiative contributions to c_{33} dominate the matrix c_{ij} and the mixing angle typically turns out to be too small to give rise to measurable effects). The interesting feature is that this structure gives rise to large mixing between the second and third family independently of how small σ is. This might give large effects in $\tau \to \mu\gamma$ transitions. However, by making σ small these effects can be kept under control. Still, the LFV effects at colliders do not get suppressed, as long as $|\tilde{m}_2 - \tilde{m}_3| \gtrsim \Gamma$ [26], where Γ is the slepton width, because the mixing angle remains large in the $\sigma \to 0$ limit. Note that collider and low energy effects ($\mathrm{BR}(\tau \to \mu\gamma)$)are complementary, as the former are interesting when $\tan\beta$ is not too large, while the latter are enhanced in the large $\tan\beta$ regime.

Let us summarize this section. We studied the predictions of the flavor model of section 2 for FCNC and LFV effects. For this, we assumed universal soft SUSY-breaking terms at a high scale $M_c > M_R$, which will be identified with the compactification scale of the full 5D model. We studied the RG evolution of the parameters to low energy for two different regimes of $\tan\beta$. The comparison with low-energy data (fermion masses and mixings) gives constraints on some of the Superpotential couplings, which are of $\mathcal{O}(1)$ as expected. All couplings which are not fixed by data are assumed to be $\mathcal{O}(1)$. We find the following results:

- in the large $\tan\beta$ regime ($\tan\beta = 53$), the present limit on $BR(\tau \to \mu\gamma)$ gives only weak constraints on the SUSY parameter space, $(m_0,\, M_{1/2}) \sim 1\,\mathrm{TeV}$, while the expected sensitivity of a Super B-Factory could probe almost completely the parameter space for SUSY masses within the LHC reach;

- for a lower value of $\tan\beta = 40$, the parameter space is presently unconstrained and will be tested by future experiments up to $(m_0,\, M_{1/2}) \sim 1\,\mathrm{TeV}$.

4 An SO(10) embedding in 5 dimensions

We now embed the PS model illustrated in section 2 in a five-dimensional, supersymmetric, SO(10) model. What follows is not the only possible embedding in a 5D unified model and as such it should be considered as a proof of existence of a unified version of the model.

The benefits of considering unification in the presence of one or more extra-dimension with an inverse size of the order of the Grand Unification Theory (GUT) scale are well

JHEP03(2009)031

known and include an easy implementation of doublet-triplet splitting and the suppression of dimension five operators contribution to proton decay [27, 28]. In our case, the presence of the fifth dimension is welcome also because it provides more freedom on the light field spectrum, which in turn helps maintaining (and in some case improving) the successful α_s prediction in the MSSM. The use of SO(10) is dictated by the need of having PS as a subgroup. Earlier work on SO(10) in five dimensions can be found in [29].

The fifth dimension is compactified on a $S^1/(Z_2 \times Z_2')$ orbifold. SO(10) is broken to $G_{\rm PS}$ on the $y = \pi R/2$ brane and unbroken on the $y = 0$ brane (R is the compactification radius, y the coordinate on the fifth dimension, $y \sim y+2\pi R$, $y \sim -y$, $y' \sim -y'$, $y' = y+\pi R/2$). The 4D $N = 2$ supersymmetry is broken to $N = 1$ supersymmetry on both the four-dimensional branes. The Z_2 parities relate the values of the fields as follows: $\Phi(x, y) = P\Phi(x, -y)$, $\Phi(x, y') = P'\Phi(x, -y')$, where $P^2 = P'^2 = 1$. In an appropriate basis, each field Φ can be classified by its eigenvalues $(\pm 1, \pm 1)$ under (P, P'). The expansion in Kaluza-Klein (KK) modes is then

$$\Phi_{++}(x, y) = \sqrt{\frac{4}{\pi R}} \sum_{n=0}^{\infty} \frac{1}{(\sqrt{2})^{\delta_{n,0}}} \Phi_{++}^{(2n)}(x) \cos \frac{2ny}{R} \tag{4.1a}$$

$$\Phi_{+-}(x, y) = \sqrt{\frac{4}{\pi R}} \sum_{n=0}^{\infty} \Phi_{+-}^{(2n+1)}(x) \cos \frac{(2n+1)y}{R} \tag{4.1b}$$

$$\Phi_{-+}(x, y) = \sqrt{\frac{4}{\pi R}} \sum_{n=0}^{\infty} \Phi_{-+}^{(2n+1)}(x) \sin \frac{(2n+1)y}{R} \tag{4.1c}$$

$$\Phi_{--}(x, y) = \sqrt{\frac{4}{\pi R}} \sum_{n=0}^{\infty} \Phi_{--}^{(2n+2)}(x) \sin \frac{(2n+2)y}{R}. \tag{4.1d}$$

As usual, only Φ_{++} and Φ_{+-} (Φ_{++} and Φ_{-+}) are possibly non-vanishing at the $y = 0$ ($y = \pi R/2$) brane and only Φ_{++} has a massless zero mode.

The supersymmetric structure can be formulated in terms of the superfield language of the unbroken four-dimensional $N = 1$ supersymmetry. The 5D vector multiplet consists of a vector and a chiral multiplet, V and Φ, while the 5D hypermultiplet decomposes into two chiral multiplets in conjugate representations, say H and $\tilde{H}$. The orbifold parities of the vector multiplet components can be chosen in such a way that $V = V_{++}^{\rm PS} + V_{+-}^{\rm SO(10)/PS}$, $\Phi = \Phi_{--}^{\rm PS} + \Phi_{-+}^{\rm SO(10)/PS}$. SO(10) is thus unbroken at $y = 0$ (the "SO(10) brane") and broken to PS at $y = \pi R/2$ (the "PS brane"), and $N = 2$ supersymmetry is broken to $N = 1$ on both branes, as anticipated. Let us now consider a bulk SO(10) hypermultiplet $(H, \tilde{H})$. In most cases H and $\tilde{H}$ split into two PS components $H = H_1 + H_2$, $\tilde{H} = \tilde{H}_1 + \tilde{H}_2$. Let H_1 be the "++" mode, $H_1 = (H_1)_{++}$. The relative orbifold parities are then dictated by the invariance of the bulk action: $H_2 = (H_2)_{+-}$, $\tilde{H}_1 = (\tilde{H}_1)_{--}$, $\tilde{H}_2 = (\tilde{H}_2)_{-+}$. All the degrees of freedom of the vector multiplet but the PS gauge bosons and gauginos get mass at the compactification scale $M_c \equiv 1/R$ or higher. Some of the fields in the effective model of section 2 are embedded in bulk fields. In this case, they correspond to the "++" (zero) modes of those fields. All the other degrees of freedom of those bulk fields get a mass at the scale $1/R$ or higher. The fields heavier than the compactification scale can be ignored

JHEP03(2009)031

	ψ_i	ψ'	$\bar{\psi}'$	F	F_c	$\bar{F}$	$\bar{F}_c$	h	ϕ	S_j	F'_c	$\bar{F}'_c$	X_c	Σ
Localization	SO(10)			bulk							PS			
Gauge repr	16	16	$\overline{16}$	16	16	$\overline{16}$	$\overline{16}$	10	45	1	$(1,2,\bar{4})$	$(1,2,4)$	$(1,3,1)$	$(1,1,15)$
$\mathrm{U}(1)_R$	1	0	0	1	1	1	1	0	0	1	0	0	0	1
Z_{24}	-7	9	1	-6	-6	-6	-6	-11	-11	6	2	2	12	4

Table 5. Embedding of the fields in table 1 in the 5D SO(10) model ($i,j=1,2,3$), localization in the fifth dimension and quantum numbers under the relevant symmetries.

	Φ	Y_{10}	Y'_{10}	H	H_6	$\theta^{\pm}$	$\Theta^{\pm}$	Y_{PS}	Y'_{PS}	x_c	x	Ω
Localization	SO(10)				bulk			PS				
Gauge repr	45	1	1	10	10	1	1	1	1	$(1,3,1)$	$(3,1,1)$	$(2,2,6)$
$\mathrm{U}(1)_R$	2	2	2	2	2	0	0	2	2	2	1	0
Z_{24}	-10	-10	0	2	1	± 3	∓ 2	-4	0	3	3	-9

Table 6. Additional fields involved in different aspects of the 5D SO(10) model

in first approximation. They will be discussed in the context of gauge coupling unification.

Let us now come to the embedding of the effective model of section 2. The PS vector fields are identified with the zero modes of V^{PS}_{++}. The fields in table 1 are embedded in the fields in table 5. The fields f_i and f^c_i, $i=1,2,3$, making up the three MSSM families in the unbroken $\mathbf{Z}_2$ limit, become the three ψ_i on the SO(10) brane. The successful SO(10) predictions of the SM fermion gauge quantum numbers is therefore maintained. The Higgs h, the $\mathbf{Z}_2$ breaking field ϕ, and the messengers F, F_c, $\bar{F}$, $\bar{F}_c$ become the zero modes of the $++$ component of the corresponding bulk fields (with an abuse of notation we denote the bulk field by the symbol that would be used for its zero mode component). The PS-breaking fields F'_c, $\bar{F}'_c$, X_c, and the $\mathrm{SU}(2)_R$-breaking messenger field Σ live on the PS brane. The spectrum in table 5 also includes 3 bulk singlets S_j, $j=1,2,3$, and the $\psi'+\bar{\psi}'$ on the SO(10) brane. The latter fields play a role in the neutrino sector.

We aim at exhibiting a full model taking care of the vevs used in the generation of the flavour structure, among the other things. The fields involved in those (implementation-dependent) "side" aspects of the model are listed in table 6. Some of them are needed, as mentioned, to generate the necessary vevs (the singlets, essentially), some to get a field content able to preserve an MSSM 1-loop unification all the way up to the unification scale [30] (H_6, x_c, x, Ω), some to avoid unwanted Goldstones and to set each field at the appropriate scale.

Tables 5 and 6 show the $\mathrm{U}(1)_R$ assignment of the fields. The $\mathrm{U}(1)_R$ symmetry we are considering is not directly related to the bulk $\mathrm{SU}(2)_R$ symmetry characterizing 5D supersymmetry. The latter is broken to a $\mathrm{U}(1)'_R$ by boundary conditions and can easily be strongly broken spontaneously. The former R-symmetry contains the R-parity symmetry

JHEP03(2009)031

R_P used in section 2.[5] It will play a role in suppressing proton decay and naturally explains why the MSSM Higgs fields stay light [27]. The discrete Z_{24} symmetry is used to constrain the superpotential and contains the $\mathbf{Z}_2$ of section 2, to which it is spontaneously broken above the scale M_R ($\mathbf{Z}_2$ is broken as needed to reproduce the results in section 2).

4.1 The strong coupling order parameter

Two nice features of the model we are proposing are the possibility to relate the $\mathcal{O}(1)$ parameters to strong couplings and the fact that some of the order parameters (all except two, as we will see) are identified with hierarchies among strong couplings involving different types of fields. In order to show this, we first introduce properly normalized, dimensionless fields.

We assume that the theory approaches a strongly interacting regime at the cutoff scale Λ. Naive dimensional analysis (NDA) suggests to write the action in terms of normalized derivatives $\hat{\partial} = \partial/\Lambda$ and of dimensionless chiral and vector superfields $\hat{\phi}$, $\hat{V}$, related to the canonically normalized fields ϕ, V by

$$\phi_4 = \hat{\phi}_4 \left(\frac{\Lambda^2}{l_4}\right)^{1/2}, \quad \phi_5 = \hat{\phi}_5 \left(\frac{\Lambda^3}{l_5}\right)^{1/2}, \quad V_4 = \hat{V}_4 \left(\frac{\Lambda^2}{l_4^V}\right)^{1/2}, \quad V_5 = \hat{V}_5 \left(\frac{\Lambda^3}{l_5^V}\right)^{1/2}, \tag{4.2}$$

where the index 4 (5) denotes brane (bulk) fields. When expressed in terms of the dimensionless fields above, the brane superpotential acquires the form

$$W_{\text{brane}}(\phi_i) = \frac{\Lambda^3}{l_4} \hat{W}(\hat{\phi}_i), \tag{4.3}$$

where $\hat{W}$ does not contain dimensionful parameters and its expansion is expected to involve $\mathcal{O}(1)$ coefficients [31].[6]

The values of the dimensionless coefficients $l_{4,5}^{(V)}$ leading to $\mathcal{O}(1)$ coefficients in $\hat{W}$ (defined of course themselves up to $\mathcal{O}(1)$ factors) depend on the theory under consideration and may be different for different fields. The guideline provided by NDA is that l_D is just the loop factor in D dimensions: $l_D = (4\pi)^{D/2}\Gamma(D/2)$. In our case, we will use the same factor l_4 (l_5) for all the chiral brane (bulk) superfields (superpotential couplings), while we keep the possibility of having a different normalization for the vector fields (gauge couplings). This is because the gauge couplings are qualitatively different in that the coefficients of the gauge loop expansion grow with the number of charged matter fields. With the field content in the tables 5 and 6, we expect l_V to be smaller by a factor $\mathcal{O}(5)$ [32].

Whatever are the precise values of the coefficients $l_{4,5}^{(V)}$, the important point for our purposes is that they lead to small hierarchies that contribute to account for the fermion mass hierarchies [33]. In practice, the relevant order parameter turns out to be

$$\lambda \equiv 1/l_4^{1/4} \approx 0.24 \approx \sqrt{\epsilon}. \tag{4.4}$$

[5] The $\mathrm{U}(1)_R$ could for example be broken together with supersymmetry down to an R-parity if the superfield breaking supersymmetry has $R = 0$.

[6] Note that the derivation in [31] assumes an infinite extra-dimension. See [32] for a more detailed approach.

JHEP03(2009)031

The numerical value is compatible with the NDA prediction for l_4. However, it is actually chosen in order to be able to best fit the numerical values in the following. The reason why this is the relevant parameter is that it enters the expected values of mass terms, as we now see. When written in terms of the dimensionless fields, the mass terms in $\hat{W}$ will be dimensionless numbers, say η. In the strong coupling regime, we expect $\eta = \mathcal{O}(1)$, but smaller values are of course allowed. In terms of canonically normalized fields, the mass term shows a dependence on λ:

$$M \sim \eta\, \lambda^{n_B} \Lambda, \tag{4.5}$$

where n_B is the number of bulk fields involved in the mass term ($n_B = 0, 1, 2$). In order to understand the above formula, one should first note that a term in $\hat{W}$ involving n_B bulk fields and n_b brane fields will give rise in this strong coupling regime to an effective 4D coupling g of order

$$g \sim \left(\frac{2l_5}{\pi R \Lambda}\right)^{n_B/2} l_4^{n_b/2-1} \tag{4.6}$$

(we neglect the running, which can be significant). The effective model in section 2 assumes the couplings to be $\mathcal{O}(1)$. Because it will turn out that those couplings come from interactions involving $n_B = 2$ bulk and $n_b = 1$ brane fields, we can write $2l_5/(\pi R\Lambda)$ as $l_4^{1/2} = 1/\lambda^2$, up to $\mathcal{O}(1)$ factors. This is why only the λ parameter enters eq. (4.5). Also, this allows to relate ΛR to $l_{4,5}$. Assuming that l_5 is such that $2l_5/\pi \sim 100$, we have $\Lambda R \sim 5$. We can check the consistency of the numbers estimating the size of the gauge couplings at the cutoff scale. This is determined by $l_5/l_5^V \sim 5$, which gives $g_{4D}^2(\Lambda) \sim l_5^V/(\lambda^2 l_5) \sim 3.5$, which is close to the (radiatively enhanced) value of g_{4D}^2 we find in section 4.5.

4.2 Brane superpotentials

The (normalized) superpotentials on the SO(10) and PS branes are

$$\hat{W}_{\mathrm{SO(10),PS}} = \hat{W}^{\mathrm{flav}}_{\mathrm{SO(10),PS}} + \hat{W}^{\mathrm{vevs}}_{\mathrm{SO(10),PS}} + \hat{W}^{\mathrm{mass}}_{\mathrm{SO(10),PS}}. \tag{4.7}$$

The $\hat{W}^{\mathrm{flav}}_{\mathrm{SO(10),PS}}$ parts are directly related to the superpotential in eq. (2.1) and therefore to the SM flavour structure. They are (keeping only "++" components of bulk fields)

$$\hat{W}^{\mathrm{flav}}_{\mathrm{SO(10)}} = \lambda_i \hat{\psi}_i \hat{F} \hat{h} + \lambda_i^c \hat{\psi}_i \hat{F}_c \hat{h} + \alpha_i \hat{\psi}_i \hat{\bar{F}} \hat{\phi} + \alpha_i^c \hat{\psi}_i \hat{\bar{F}}_c \hat{\phi} + a_{ij} \hat{\bar{\psi}}' \hat{S}_i \hat{\psi}_j, \tag{4.8a}$$

$$\hat{W}^{\mathrm{flav}}_{\mathrm{PS}} = a \hat{\bar{F}}_c \hat{X}_c \hat{F}_c + \bar{\sigma}_c \hat{\bar{F}}'_c \hat{\Sigma} \hat{F}_c + \sigma_c \hat{\bar{F}}_c \hat{\Sigma} \hat{F}'_c + b \frac{\hat{F}'_c \hat{X}_c \hat{F}'_c}{2} \hat{\Sigma}^2 + b_i \hat{\bar{F}}'_c \hat{S}_i \hat{F}_c \hat{\Theta}_+ + c_i \hat{\bar{F}}_c \hat{S}_i \hat{F}'_c \hat{\Theta}_+. \tag{4.8b}$$

The last terms affect the singlet neutrino mass matrix. All couplings are $\mathcal{O}(1)$, as predicted by the strong coupling assumption. Despite the same notation, they are not exactly the same as the corresponding parameters in eq. (2.1), but the difference is an irrelevant $\mathcal{O}(1)$ factor.

Some of the $R = 0$ fields in the superpotentials above get a vev due to (here and below we omit $\mathcal{O}(1)$ coefficients)

$$\hat{W}^{\mathrm{vevs}}_{\mathrm{SO(10)}} = \hat{Y}_{10} \left(\hat{\bar{\psi}}' \psi' - \hat{\theta}_+^2 \hat{\Theta}_-^2\right) + \hat{Y}'_{10} \left(\hat{\theta}_+ \hat{\theta}_- - \epsilon_{10}^2\right) + \hat{\bar{\psi}}' \hat{\Phi}\, \hat{\psi}' + \hat{\theta}_- \hat{\phi}\, \hat{\Phi}, \tag{4.9a}$$

$$\hat{W}^{\mathrm{vevs}}_{\mathrm{PS}} = \hat{Y}_{\mathrm{PS}} \left(\hat{\bar{F}}'_c \hat{F}'_c - \hat{\Theta}_-^2\right) + \hat{Y}'_{\mathrm{PS}} \left(\hat{\Theta}_+ \hat{\Theta}_- - \epsilon_{\mathrm{PS}}^2\right) + \hat{\theta}_- \hat{\Theta}_+^2 \hat{\bar{F}}'_c\, \hat{x}_c \hat{F}'_c + \hat{\theta}_+ \hat{\Theta}_-^3 \hat{x}_c\, \hat{X}_c. \tag{4.9b}$$

The superpotentials above contain two anomalously small coefficients $\epsilon_{\rm PS} \sim \lambda$ and $\epsilon_{10} \sim \lambda^2$ characterizing the PS and SO(10) branes respectively. Together with the dynamically generated λ, $\epsilon_{\rm PS}$ and ϵ_{10} are the seeds of the fermion hierarchies. It is tempting to generate dynamically $\epsilon_{\rm PS}$ and ϵ_{10} in terms of λ, but this is beyond the scope of this paper. Another aspect of the model that is left to further investigation is the suppression of the mass term arising from the vev of the $SU(2)_R$-triplet component of ϕ in eq. (4.8). This suppression is necessary in order to preserve the m_μ/m_s ratio obtained in section 2. The F-term equations give

$$\langle \hat{\Theta}_\pm \rangle \sim \langle \hat{F}'_c \rangle \sim \langle \hat{\bar{F}}'_c \rangle \sim \langle \hat{X}_c \rangle \sim \lambda, \qquad \langle \hat{\theta}_\pm \rangle \sim \lambda^2, \qquad \langle \hat{\psi}' \rangle \sim \langle \hat{\bar{\psi}}' \rangle \sim \lambda^3, \qquad \langle \hat{\phi} \rangle \sim \lambda^4. \tag{4.10}$$

Finally, we need to provide mass terms for some otherwise light fields. These are provided by

$$\hat{W}_{\rm PS}^{\rm mass} = \hat{\theta}_- \hat{\Theta}_+ \hat{\bar{F}}'_c \hat{\bar{F}}'_c \hat{H}_6 + \hat{\theta}_- \hat{\Theta}_+ \hat{F}'_c \hat{F}'_c \hat{H}_6 + \frac{\hat{\Theta}_+^3}{2} \hat{x}^2 + \hat{\psi}' \hat{\psi}' \hat{H} \hat{\Theta}_-^2 + \hat{\bar{\psi}}' \hat{\bar{\psi}}' \hat{H} \hat{\Theta}_+^2. \tag{4.11}$$

Also relevant are two operators involving fields with no zero mode. The bulk field we denoted by ϕ is an hypermultiplet corresponding to 4 PS bulk fields with different orbifold parities: $(\phi_{\rm PS})_{++}$, the field whose zero mode enters eq. (2.1), $(\phi_{226})_{+-}$, its SO(10) complement, and the conjugated fields $(\tilde{\phi}_{\rm PS})_{--}$ and $(\tilde{\phi}_{226})_{-+}$. The operators $(\phi_{226})_{+-}$ and $(\tilde{\phi}_{226})_{-+}$ have no zero mode but they are relevant for our purposes. They appear in fact in the following two operators: $\hat{\Omega}\hat{\Theta}_+(\hat{\tilde{\phi}}_{226})_{-+}$, on the PS brane, and $\hat{\Phi}_{226}\hat{\theta}_-(\hat{\phi}_{226})_{+-}$, on the SO(10) brane. When integrating out the heavy $(\tilde{\phi}_{226})_{-+}$, $(\phi_{226})_{+-}$ fields, one obtains the operator $\hat{\Theta}_+\hat{\theta}_-\hat{\Omega}\hat{\Phi}_{226}$, involving fields from two different branes.[7] The latter gives a mass term at the scale M_R coupling the fields Ω and Φ_{226}.

4.3 Scales, spectrum, and unification

We now illustrate the spectrum we obtain for the heavy fields and in particular we relate the scales M_R and M_L of the right- and left-handed messengers defined in section 2 to the cutoff Λ. In order to do that, we make an extensive use of eq. (4.5).

We take $\Lambda \approx 10^{17}\,\text{GeV}$. The right-handed messengers in F_c, $\bar{F}_c$, as well as Σ, get a mass

$$\mathcal{O}\left(\lambda^3 \Lambda\right) \sim 2 \cdot 10^{15}\,\text{GeV} \equiv M_R. \tag{4.12}$$

The up quark sector involves a mixed mass term arising from the vevs of F'_c, $\bar{F}'_c$, which is enhanced by a factor $1/\lambda$, $V_c \sim M_R/\lambda \approx M_R/\sqrt{\epsilon}$. As discussed in section 2, such an enhancement accounts for the smallness of m_c/m_t (and will give a threshold correction to gauge coupling unification). The masses M_R and V_c are different despite they arise from dimensionless vevs of the same order because the corresponding mass terms contain a different number of bulk fields, in agreement with eq. (4.5).

[7] Let b_i^{10}, $i = 1 \ldots h$ be SO(10) brane fields, $b_j^{\rm PS}$, $j = 1 \ldots k$ be PS brane fields and B be a bulk field. After integrating out the heavy bulk fields, the operators $a_{10}\hat{b}_1^{10} \ldots \hat{b}_h^{10}\hat{B}_{(+,-)}$ and $a_{\rm PS}\hat{b}_1^{\rm PS} \ldots \hat{b}_k^{\rm PS}\hat{\bar{B}}_{(-+)}$ on the two branes give rise to the effective interaction $a_{10}a_{\rm PS}\hat{b}_1^{10} \ldots \hat{b}_h^{10}\hat{b}_1^{\rm PS} \ldots \hat{b}_k^{\rm PS}$.

JHEP03(2009)031

Once $\mathbf{Z}_2$ is broken by the vev of ϕ, the messengers and the would be light families get mixed by a mass term

$$\mathcal{O}\left(\lambda^5\Lambda\right) \sim 3 \cdot 10^{14}\,\mathrm{GeV} \equiv M_L, \tag{4.13}$$

so that $\epsilon = M_L/M_R \approx \lambda^2 \approx 0.06$. The two mass terms mixing the singlets S_i with N_c and n_i^c are both $\mathcal{O}\left(\lambda M_R\right)$, half way between M_L and M_R.

Below the compactification scale $M_c = 1/R$, SO(10) is broken to PS and the spectrum is made of the PS vector fields, the brane fields, and the zero modes of the bulk fields in the tables 5 and 6. It is interesting (although in part cooked up) that this constitutes a retarding PS "magic" field content, with the terminology of [30]. This means that such a field content would exactly preserve (but delay to a higher GUT scale) a MSSM 1-loop gauge coupling unification, despite the field content does not correspond to a complete SU(5) representation. A systematic study of such "magic" field contents can be found in [30]. We will make extensive use of such contents in the following.

Let us now consider the situation below the scale M_R, where the PS group is broken to the SM one and the right-handed messengers decouple. The (non-singlet) fields are: the SM fields; the left-messengers $\bar{L}L + \bar{Q}Q$; 2 right-handed lepton-like components (and their conjugates) in x_c and F_c',$\bar{F}_c'$; 2 right-handed down quark-like components (and their conjugates) in H_6 and F_c',$\bar{F}_c'$; linear combinations of the up quark-like and singlet lepton-like components in ϕ and ψ' (and their conjugates); linear combination of the quark-doublet like components in ϕ and Ω (and their conjugates); the fields contained in the 5 and $\bar{5}$ SU(5) components of $\bar{\psi}'$, ψ' and H. What matters for our purposes is that this also turns out to be a magic field content, with equal contributions to all beta-function coefficients, and thus it is not changing the unification scale.

Below M_L, only the SM fields (and possibly a set of full SU(5) multiplets) are supposed to survive. This needs $\mathcal{O}\left(M_L\right)$ $\mathrm{U}(1)_R$-breaking mass terms for the linear combinations involving ψ', ϕ and Ω mentioned above, which constitutes a full 10 and $\overline{10}$ of SU(5). It is not difficult to arrange a superpotential involving a $R = 2$ singlet getting a vev at the scale $\mathcal{O}\left(M_L\right) = \mathcal{O}\left(\lambda^5\Lambda\right)$.

To summarize, we have the following scales: $\Lambda \approx M_{\mathrm{GUT}} \approx 10^{17}\,\mathrm{GeV}$, $M_c = 1/R \approx 2 \cdot 10^{16}\,\mathrm{GeV}$, $M_R \approx \lambda^3\Lambda \approx 2 \cdot 10^{15}\,\mathrm{GeV}$, $M_L \approx \lambda^5\Lambda \approx 3 \cdot 10^{14}\,\mathrm{GeV}$ and a magic field set from Λ down to the electroweak scale except for a small threshold.

4.4 Neutrinos

The light neutrino mass matrix originates from the NR operator $h_{ij}(l_i' h_u)(l_j' h_u)/(2\Lambda_L)$, where $l_{1,2,3}'$ are the three light lepton doublet mass eigenstates: $m_{ij}^\nu = h_{ij} v_u^2/\Lambda_L$. The coefficients h_{ij}/Λ_L are obtained by integrating out the R_P-odd heavy singlet neutrinos.

We aim at obtaining a large atmospheric angle θ_{23}, the atmospheric squared mass difference Δm_{23}^2 at the correct scale, and the suppression of the solar squared mass difference Δm_{12}^2 (in the context of normal hierarchical neutrinos) and of the θ_{13} angle. Previously [1], the large atmospheric angle and the $\Delta m_{12}^2/\Delta m_{23}^2$ suppression were obtained essentially through the single right-handed neutrino dominance mechanism. In fact, the whole idea underlying this flavour model, based on the exchange of a single family of flavour

JHEP03(2009)031

messengers, can be considered as an extension of that mechanism. In order to reproduce the single right-handed neutrino dominance mechanism, the left-handed messengers should have a mass term at the M_L scale (along the $B-L$ direction). Here, we prefer to consider the more economical option in which a such term does not arise or arises at a lower scale. This is interesting also because the large atmospheric mixing arises through a different, unusual mechanism, as we are now going to see.

In our model, the singlet neutrinos taking part to the see-saw are more numerous than the usual 3. There are in fact 9 R_P-odd singlet neutrino fields in the model. These are the usual three right-handed neutrinos n_i^c, the $\mathrm{SU}(2)_R$ partners of the SM right-handed charged fermions e_i^c. In addition, there are N^c, $\bar{N}^c$, [8] A_Σ, and three gauge singlets S_i (additional singlets do not play a role as they have different R_P, do not mix with the previous ones, and are not relevant for light neutrino masses). The heavy singlet neutrino mass terms are given by $-(N^c, \bar{N}^c, A_\Sigma, n_i^c, S_k)^T M_s (N^c, \bar{N}^c, A_\Sigma, n_j^c, S_h)/2$, where

$$M_s = \begin{pmatrix} 0 & M_R & \sqrt{\frac{3}{8}}\bar{\sigma}_c \bar{V}_c & 0 & b_h M_{SN} \\ M_R & 0 & \sqrt{\frac{3}{8}}\sigma_c V_c & \alpha_j^c v & c_h M_{SN} \\ \sqrt{\frac{3}{8}}\bar{\sigma}_c \bar{V}_c & \sqrt{\frac{3}{8}}\sigma_c V^c & M_\Sigma & 0 & 0 \\ 0 & \alpha_i^c v & 0 & 0 & a_{ih} M_{Sn} \\ b_k M_{SN} & c_k M_{SN} & 0 & a_{kj} M_{Sn} & 0 \end{pmatrix} \tag{4.14}$$

and the light neutrino mass operator is

$$\frac{h_{ij}}{2\Lambda_L}\left(l_i' h_u\right)\left(l_j' h_u\right) = \frac{1}{2}\Big[\left(M_s^{-1}\right)_{N^c N^c}\left(\lambda_2^c l_2'\right)^2 + \left(M_s^{-1}\right)_{n_3^c n_3^c}\left(\lambda_3 l_3'\right)^2 + 2\left(M_s^{-1}\right)_{N^c n_3^c}\left(\lambda_2^c l_2'\right)\left(\lambda_3 l_3'\right)\Big] h_u^2, \tag{4.15}$$

so that

$$m_\nu = v_u^2 \begin{pmatrix} 0 & 0 & 0 \\ 0 & (\lambda_2^c)^2 (M_s^{-1})_{N^c N^c} & \lambda_2^c \lambda_3 (M_s^{-1})_{N^c n_3^c} \\ 0 & \lambda_2^c \lambda_3 (M_s^{-1})_{N^c n_3^c} & \lambda_3^2 (M_s^{-1})_{n_3^c n_3^c} \end{pmatrix}. \tag{4.16}$$

The entries in the first row and column, accounting for the solar and θ_{13} mixing angles, will be generated, as in the case of charged fermion masses, by higher order operators, possibly controlled by a flavour symmetry. In eq. (4.14) the entries set to zero arise at a negligible level.

In order to get a large atmospheric mixing angle from eq. (4.16), we need $(M_s^{-1})_{N^c N^c} \sim (M_s^{-1})_{N^c n^c} \sim (M_s^{-1})_{n^c n^c}$ and in order to obtain the (mild) hierarchy between the solar and atmospheric squared mass differences, we need the determinant $(M_s^{-1})_{N^c N^c}(M_s^{-1})_{n^c n^c} - (M_s^{-1})^2_{N^c n^c}$ to be suppressed. This can be obtained if $M_{SN} \sim M_{Sn} > M_L$, in which case

$$(M_s^{-1})_{N^c N^c} \sim (M_s^{-1})_{N^c n_3^c} \sim (M_s^{-1})_{n_3^c n_3^c} \sim \frac{1}{2M_R} \tag{4.18}$$

[8] It is sufficient to consider only the KK zero-modes of N^c and $\bar{N}^c$, because their mass terms arise purely from the PS brane. That means that higher KK mode pairs $(++,--)_{n>0}$ and $(+-,-+)_{n\geq 0}$ decouple from the other fields, because one member of these pairs vanishes at the PS brane and has therefore only a heavy mass term with its partner.

JHEP03(2009)031

$$(M_s^{-1})_{N^cN^c}(M_s^{-1})_{n_3^cn_3^c} - (M_s^{-1})^2_{N^cn_3^c} \sim \frac{M_R^2}{V_c^2}(M_s^{-1})^2_{N^cN^c}. \tag{4.19}$$

This is indeed what our model gives: $M_{SN} \sim M_{Sn} \sim \lambda M_R > \lambda^2 M_R \sim M_L$ and $M_R/V_c \sim \lambda < 1$.

Taking into account all $\mathcal{O}(1)$ coefficients we finally obtain for the light neutrino masses and the atmospheric mixing

$$m_3 = \frac{v_h^2}{M_R}\frac{A}{2\sin^2\theta_{23}} \tag{4.21}$$

$$\frac{m_2}{m_3} = \frac{4\lambda^2}{3}\sin^2 2\theta_{23} B \tag{4.22}$$

$$\tan\theta_{23} = C, \tag{4.23}$$

where

$$A = \frac{(\lambda_2^c)^2\sigma_c}{\bar{\sigma}_c}, \qquad B = \frac{\bar{\sigma}_c x^2}{\sigma_c y^2}, \qquad C = \frac{\lambda_2^c \sigma_c \det a}{\lambda_3 y} \tag{4.25}$$

$$x = c_2\left(a_{12}a_{31} - a_{11}a_{32}\right) + c_3\left(a_{11}a_{22} - a_{12}a_{21}\right) \tag{4.26}$$

$$y = \bar{\sigma}_c x - \sigma_c b_3\left(a_{11}a_{22} - a_{12}a_{21}\right). \tag{4.27}$$

In order to agree with the experimental values $m_2/m_3 \approx \sqrt{\Delta m_{12}^2/\Delta m_{23}^2} \sim 0.2$ and $\tan\theta_{23} \sim 1$, one has to require that the above functions of $\mathcal{O}(1)$ coefficients take the (reasonable) values $B \sim 3$ and $C \sim 1$. The atmospheric squared mass difference provides an experimental determination of $m_3 \approx \sqrt{\Delta m_{23}^2}$, which translates into a determination of the scale M_R, given by

$$M_R = \frac{v_h^2 A}{2\cos^2\theta_{23}\sqrt{\Delta m_{23}^2}} \sim A \times 6 \times 10^{14}\text{GeV}. \tag{4.28}$$

To achieve agreement with the numerical determination of the various scales provided by gauge coupling unification, we have to require that $A \approx 3$.

4.5 Gauge coupling unification

In the context of the 5D model under consideration, gauge coupling unification has novel features. A generic feature of 5D models is the presence of threshold effects associated to the tower of KK excitations associated to bulk fields (sometimes useful to improve the gauge coupling unification prediction). In our case such thresholds do not arise at the 1-loop level.

The reason why the KK threshold corrections are typically present in 5D models is that the very breaking of the unified group by boundary conditions also splits the multiplets associated to the fields in the bulk into submultiplets that are not full representations of the gauge group and have different masses. In our case, however, such non-full representations happen again to preserve MSSM 1-loop unification at each floor of the KK tower (and do not affect the unification scale).

JHEP03(2009)031

The beta function coefficients at one loop, neglecting the threshold effects associated to $V_c > M_R$, follow. Below M_L the coefficients are the MSSM ones: $(b_1, b_2, b_3) = (33/5, 1, -3)$. The quantity determining the α_s prediction at one loop is $(b_3 - b_2)/(b_1 - b_2) = -5/7$. In our case, the content of fields between M_L and M_R gives a common shift to the coefficients, even if the new fields are not in full SU(5) multiplets, so that the condition above is trivially satisfied. The coefficients are $(b_1, b_2, b_3) = (78/5, 10, 6)$. The 1-loop MSSM α_3 prediction is preserved independently of the value of the scale M_L. Above M_R the gauge group is $G_{\rm PS}$, the SM gauge couplings are matched into the PS ones by

$$\frac{1}{\alpha_4} = \frac{1}{\alpha_3}, \qquad \frac{1}{\alpha_L} = \frac{1}{\alpha_2}, \qquad \frac{1}{\alpha_R} = \frac{5}{3}\frac{1}{\alpha_1} - \frac{2}{3}\frac{1}{\alpha_3}, \tag{4.29}$$

and the 1-loop MSSM α_3 prediction is preserved if $(b_4 - b_L)/(b_R - b_L) = -1/3$. This is indeed what happens. In fact, between M_R and $1/R$ we have $(b_L, b_R, b_4) = (28, 34, 26)$ and above $1/R$ each KK set adds $(b_L, b_R, b_4) = (10, 10, 10)$. The coefficients associated to the KK floors are the same for the three gauge couplings but still they do not correspond to full SU(5) multiplets. The 4D gauge couplings are supposed to unify at the cutoff Λ within an intrinsic uncertainty due to unknown brane Yang-Mills terms [27, 28]. The latter are suppressed because of the strong coupling regime assumption. The correction to $g^2(\Lambda)$ is of order $1/l_4^V$ and is therefore expected to be a few percent.

We are now in the position to calculate the prediction for $\alpha_s(M_Z)$ and $\Lambda = M_{\rm GUT}$ in our model and to discuss perturbativity, which we do in the limit in which the brane corrections vanish. We quote our results in terms of $\alpha_s^{-1}(M_Z) - \alpha_s^{-1}(M_Z)^{\rm MSSM}$ and $\Lambda/M_{\rm GUT}^{\rm MSSM}$, as the latter quantities can be calculated with a good accuracy at the one loop level (the MSSM thresholds and the 2-loop effects below M_L mostly cancel). Neglecting high energy thresholds due to small differences among the masses of the fields that were assumed to be at the M_L, M_R, or n/R scale, we have $\alpha_s(M_Z) = \alpha_s(M_Z)^{\rm MSSM}$ and $\Lambda = (M_{\rm GUT}^{\rm MSSM})^2/M_R$. The largest threshold effects come from the fact that some of the fields actually live at the scale $V_c > M_R$ or slightly below. More precisely, there are two additional thresholds corresponding to the non singlet PS/SM vector bosons. Their masses are denoted by M_E (for the $\mathrm{SU}(2)_R$ extra bosons) and M_U (for the $\mathrm{SU}(4)_c$ extra bosons). Numerically such splittings are approximately $M_E/M_R \sim 2$, $M_U/M_R \sim 1.2$. In the presence of such thresholds we have:

$$\alpha_s^{-1}(M_Z) - \alpha_s^{-1}(M_Z)^{\rm MSSM} = \frac{45}{14\pi}\log\frac{M_U}{M_R} + \frac{18}{14\pi}\log\frac{M_E}{M_R} - \frac{30}{14\pi}\log\frac{V_c}{M_R}, \tag{4.31}$$

$$\Lambda = \frac{\left(M_{\rm GUT}^{\rm MSSM}\right)^2}{M_R}\left(\frac{V_c}{M_R}\right)^{8/7}\left(\frac{M_R}{M_U}\right)^{12/7}\left(\frac{M_R}{M_E}\right)^{9/7}. \tag{4.32}$$

The correlation between the threshold effects in α_s and Λ is shown figure 5a, where the predictions for $\Lambda/M_{\rm GUT}^{\rm MSSM}$ and $\alpha_3(M_Z) - \alpha_3^{\rm MSSM}(MZ)$ are plotted for M_E and M_U randomly chosen in the ranges $1 \le M_E/M_R \le 3$, $1 \le M_U/M_R \le 3$ and V_c/M_R is varied by 50% around the central value $1/\lambda$ (all with uniform distribution in logarithmic scale). We used $\Lambda/M_R = 0.5/\lambda^3$, $M_R/M_L = 0.5/\lambda^2$ and $\Lambda R = 4$. The figure shows that it is possible to reduce the MSSM prediction for $\alpha_s(M_Z)$ while keeping Λ above $M_{\rm GUT}^{\rm MSSM}$, which helps

JHEP03(2009)031

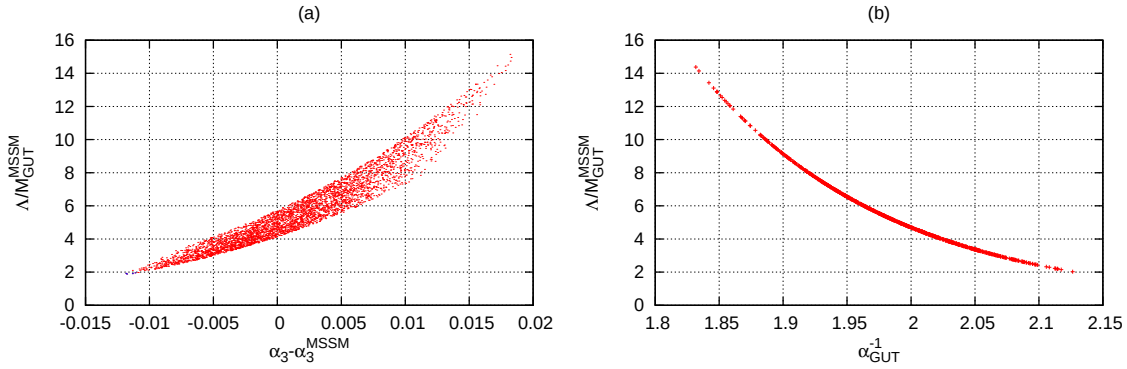

Figure 5. Correlation between the threshold effects on $\alpha_s(M_Z)$ and Λ (left). Value of $\alpha_{\rm GUT}$ at the cutoff scale (right).

with proton decay, as we will see in section 4.6. Note that a few KK masses n/R enter the running before the cutoff Λ is reached. Given the presence of so many new degrees of freedom, it is important to check that the theory (in particular the running of gauge couplings) remains calculable up to the cutoff scale. This is indeed the case, as shown in figure 5b.

4.6 Proton decay

In 4D GUTs the leading contributions to proton decay usually come from d=5 operators (via Higgs triplet exchange), while d=6 operators (via extra gauge boson exchange) are subleading. In 5D orbifold GUT models one generally finds the opposite picture: d=5 operators are strongly suppressed due to the $\mathrm{U}(1)_R$ symmetry, while d=6 operators are more important because the mass of the extra gauge bosons is smaller than in 4D GUTs ($M_c < M_{\rm GUT}^{\rm MSSM}$). This general picture also holds in our model. The dominant contribution to proton decay is SO(10)/PS gauge boson exchange, leading to a lower bound on the compactification scale $M_c > \mathcal{O}\left(10^{16}\right)$ GeV. Before deriving this bound, we briefly comment on the suppression of the d=5 operators.

The low energy effective theory below M_L is the MSSM with R-parity. This allows only for two d=5 operators that induce proton decay (originating from exchange of chiral superfields with standard model quantum numbers $(3,1)_{-1/3}$) [34],

$$QQQL|_{\theta^2} \qquad \text{and} \qquad D^c U^c U^c E^c|_{\theta^2}. \tag{4.33}$$

The operators in eq. (4.33) are suppressed because they violate the $\mathrm{U}(1)_R$ symmetry. Despite there is a source of $\mathrm{U}(1)_R$ breaking at the scale M_L (which is needed to provide the mass term $\psi'\bar{\psi}'$), it violates $\mathrm{U}(1)_R$ by +2 units and hence cannot induce the above operators. Therefore they can be assumed to be generated at the SUSY breaking scale and hence to be strongly suppressed. For the case of a minimal SUSY breaking sector (i.e. just involving a spurion with F-term vev and $R = 0$), the d=5 operators are clearly subleading.

JHEP03(2009)031

Let us now consider the d=6 operators inducing proton decay. There are two such operators in the MSSM:

$$QQ(U^c)^\dagger(E^c)^\dagger|_{\theta^4} = u_L d_L \bar{u}^c_R \bar{e}^c_R \qquad \text{and} \qquad QL(U^c)^\dagger(D^c)^\dagger|_{\theta^4} = u_L e_L \bar{u}^c_R \bar{d}^c_R. \tag{4.34}$$

These operators arise from the exchange of gauge fields with quantum numbers $(3,2)_{(5/6)}$ and $(3,2)_{(1/6)}$, which are contained in the decomposition of the SO(10)/PS gauge bosons $V^{(226)}_{+-}$. Therefore the suppression of the d=6 operators is $\mathcal{O}\left(1/M_c^2\right)$. The numerical coefficients can be calculated in close analogy to the SU(5) case [35], as we are going to show in the following.

We start with the relevant part of the 5d action

$$S_5 = \int d^4x \int_0^{\pi R/2} dy \left(\frac{1}{2g_5^2} \mathrm{Tr}\left(W^2|_{\theta^2} + \mathrm{h.c.} + 4\partial_5 V \partial_5 V|_{\theta^4}\right) + \delta(y)\psi_i^\dagger e^{2V}\psi_i|_{\theta^4} \right), \tag{4.35}$$

which fixes the normalization in the KK expansion of $V^{(226)}_{+-}$:

$$V_{+-}(x,y) = \sqrt{2}\sum_{n=0}^{\infty} V^{(2n+1)}_{+-}(x)\cos\frac{(2n+1)y}{R}. \tag{4.36}$$

The 4D effective Lagrangian is given by

$$\mathcal{L}_4 = \frac{2}{g_4^2}\sum_{n=0}^{\infty}\left(\frac{2n+1}{R}\right)^2 \mathrm{Tr}\left(V^{(2n+1)}_{+-}V^{(2n+1)}_{+-}\right) + 2\sqrt{2}\left(\psi_i^\dagger \sum_{n=0}^{\infty} V^{(2n+1)}_{+-}\psi_i\right)|_{\theta^4} \tag{4.37}$$

where we have used $1/g_4^2 = (\pi R/2)/g_5^2$. Integrating out the heavy gauge bosons, we obtain the following effective Lagrangian containing the operators in eq. (4.34)

$$\mathcal{L}_4 = \frac{g_4^2}{M_c^2}\frac{\pi^2}{4}\left(2u_l d_l \bar{u}^c_R \bar{e}^c_R + 2u_l e_l \bar{u}^c_R \bar{d}^c_R\right), \tag{4.38}$$

which is the result for an ordinary 4D SO(10) GUT with gauge boson mass given by M_c, enhanced by the $\pi^2/4$ factor, which arises from summing over KK states. The proton decay rate into $\pi^0 e^+$ follows [36]:

$$\Gamma(p\to\pi^0 e^+) = 8\alpha_H^2\frac{\pi^4}{16}\left(\frac{g_4(M_c)^2 A_R}{M_c^2}\right)^2 \frac{m_p}{64\pi f_\pi^2}\left(1+D+F\right)^2. \tag{4.39}$$

Using the hadronic parameter $\alpha_H = 0.015$ GeV^3, the pion decay constant $f_\pi = 0.13$ GeV and the chiral perturbation theory parameters $D = 0.80$ and $F = 0.47$, the partial lifetime can be estimated to be

$$1/\Gamma(p\to\pi^0 e^+) \approx 2.0\times 10^{33}\left(\frac{\alpha_4(M_c)}{1/12}\right)^{-2}\left(\frac{A_R}{2.5}\right)^{-2}\left(\frac{M_c}{10^{16}\mathrm{GeV}}\right)^4 \text{years}, \tag{4.40}$$

where the normalization uses the typical values of the gauge coupling at M_c and of the renormalization coefficient A_R we obtain in the model. A comparison with the PDG bound on the partial lifetime [37]

$$1/\Gamma(p\to\pi^0 e^+) > 1.6\times 10^{33}\text{years}, \tag{4.41}$$

JHEP03(2009)031

gives the limit we anticipated for the compactification scale

$$M_c > 9.5 \times 10^{15}\,\text{GeV} \left(\frac{\alpha_4(M_c)}{1/12}\right)^{1/2} \left(\frac{A_R}{2.5}\right)^{1/2}. \tag{4.42}$$

For $M_c \sim 2 \times 10^{16}$ GeV, the lifetime turns out to be

$$1/\Gamma(p \to \pi^0 e^+) \sim 3 \times 10^{34}\text{years}, \tag{4.43}$$

within the sensitivity of future experiments designed to reach a limit on the partial lifetime of $\mathcal{O}\left(10^{35}\right)$ years [38].

4.7 The first family

We have seen that most features of the SM fermion spectrum concerning the second and third fermion families can be accounted for without flavour symmetries or other dynamics related to the fermion family indices. The smallness of the first family charged fermion masses with respect to two heavier ones is also explained. On the other hand, in order to account for the quantitative aspects of the spectrum associated to the first family, it may be necessary to introduce some type of flavour dynamics. In this section, we sketch the case of a flavour symmetry that only acts on the first family, the second and third families being not charged.

Before showing one example of such a symmetry, let us discuss what type of Yukawa texture it should provide. One important guideline on the first family entries of the Yukawa matrices is given by the constraints from FCNC and LFV effects. Such effects are induced by off-diagonal elements in the sfermion mass matrices written in the so-called SCKM basis, the basis in which the Yukawa matrices of the corresponding fermions are diagonal. For example, eq. (3.2) gives

$$(m^2_{RR})_{\text{SCKM}} = U_R \begin{pmatrix} (m^2_{\tilde{e^c}})_{11} & 0 & 0 \\ 0 & (m^2_{\tilde{e^c}})_{22} & (m^2_{\tilde{e^c}})_{23} \\ 0 & (m^2_{\tilde{e^c}})_{23} & (m^2_{\tilde{e^c}})_{33} \end{pmatrix} U_R^\dagger, \tag{4.44}$$

$$(m^2_{LL})_{\text{SCKM}} = U_L \begin{pmatrix} (m^2_{\tilde{l}})_{11} & 0 & 0 \\ 0 & (m^2_{\tilde{l}})_{22} & 0 \\ 0 & 0 & m^2_{\tilde{L}} \end{pmatrix} U_L^\dagger \tag{4.45}$$

in the slepton sector, where U_L and U_R are the unitary matrices diagonalizing the charged lepton Yukawa matrices, $Y^E = U_R^\dagger Y^E_{\text{diag}} U_L$. Because of the sizable non-degeneracy between m^2_{11} and m^2_{22}, see eq. (3.1), a small rotation between the first two families in U_L or U_R induces a sizable off-diagonal 12 entry in m^2_{SCKM}. This in turn gives sizable contributions to the $\mu \to e\gamma$ branching ratio. Therefore, the matrices U_L and U_R should involve small rotations in the "12" block, which translates into small 12 and 21 entries in the Yukawa matrices. Analogous considerations hold in the down quark sector because of the constraints from the Kaon system (ΔM_K and ϵ_K).

Because of the above constraints and of the stronger hierarchy $m_u/m_t \ll m_d/m_b$, i) the d-quark and electron masses must originate from Y^D_{11} and Y^E_{11} respectively, ii) the

JHEP03(2009)031

corresponding up quark Yukawa should be smaller, $Y^U_{11} \ll Y^{D,E}_{11}$, and iii) the V_{us} angle must originate from the Y^U_{21}, with $Y^D_{12,21}$ and $Y^E_{12,21}$ smaller than the corresponding 11 elements.

Let us now see how the above requirements can be satisfied. The Yukawa entries $Y^{D,E}_{11}$ can be generated by the operator $\hat{\psi}_1\hat{\psi}_1\hat{\phi}\hat{h}\hat{Z}$ in the SO(10)-brane superpotential, where Z is an SO(10) adjoint living on the SO(10) brane and taking a vev in the SU(5)-invariant direction, with Z_{24} charge 12, R-charge zero, and $\langle\hat{Z}\rangle \sim \lambda^2$. After plugging the vevs of ϕ and Z and using eqs. (4.6) to write the operator in terms of canonically normalized fields, we get $Y^{D,E}_{11} \sim \lambda^5$, which is about what needed.[9] The interesting property of the operator $\hat{\psi}_1\hat{\psi}_1\hat{\phi}\hat{h}\hat{Z}$ is that it does not give rise to a contribution to Y^U_{11}, as desired. The reason can be understood as follows. The operator $\hat{\psi}_1\hat{\psi}_1\hat{\phi}\hat{h}$ does not contribute to any SM Yukawa because the vev of ϕ in the $B-L$ direction makes it antisymmetric in the two ψ's. In the case of the up quark Yukawas, the antisymmetry is not spoiled by the presence of $\hat{Z}$. This is because both the right-handed and left-handed up quarks belong to the same representation of SU(5), so that the vev of Z factorizes. Therefore the up quark Yukawa still vanishes when $\hat{Z}$ is included in the operator. On the other hand, in the case of the down quark and charged lepton Yukawas, the antisymmetry of $\psi_1\hat{\psi}_1\hat{\phi}\hat{h}$ is spoiled by the presence of $\hat{Z}$, as the right-handed and left-handed fields in this case belong to different SU(5) representations, and the vev of Z cannot be factorized. Therefore, the corresponding Yukawas do not vanish when $\hat{Z}$ is included in the operator. As for V_{us}, we said above that it should be generated by the Y^U_{21} matrix element. The latter can be generated at the correct level by the operator $\hat{\Sigma}\hat{\psi}_1\hat{h}\hat{F}'_c\hat{Z}$. This operator involves fields belonging to two different branes and can be generated by the exchange of bulk fields with no zero modes (specifically the SO(10) partner of F and its $SU(2)_R$ conjugated partner) along the lines of footnote 7. Once the vevs of $\hat{F}'_c$ and $\hat{Z}$ have been plugged, Σ has been substituted by its light $u^{c\prime}_2$ component (from eq. (2.2c) one finds that the latter is suppressed by a factor λ^3, $\bar{T}_\Sigma \sim \lambda^3 u^{c\prime}_2 + \text{heavy}$), and the "brane-brane-bulk" enhancement in footnote 9 has been taken into account, one gets $\lambda^U_{21} \sim \lambda^5$, which is about what needed to account for V_{us}.

As discussed above, if the operator $\hat{\psi}_1\hat{\psi}_1\hat{\phi}\hat{h}\hat{Z}$ was accompanied by the operator $\hat{\psi}_2\hat{\psi}_1\hat{\phi}\hat{h}\hat{Z}$, potentially dangerous FCNC and LFV effects could be generated. In order to be on the safe side and forbid the second operator one can consider a U(1) flavour symmetry under which $\psi_{2,3}$ are not charged, as promised, and ψ_1 has charge 1. Giving the Z field U(1) charge -2 allows the first operator while forbidding the second one. Such a symmetry would also forbid the $\hat{\Sigma}\hat{\psi}_1\hat{h}\hat{F}'_c\hat{Z}$ operator, as there is no U(1) assignment to Σ compatible with eq. (4.8). In order to use the U(1) symmetry above one should then use a different operator, $\hat{\Sigma}\hat{\psi}_1\hat{h}\hat{F}''_c\hat{Z}$, involving a new field F''_c on the PS brane having same gauge, Z_{24}, $U(1)_R$ charges but U(1) charge 1 (accompanied by a corresponding F field in order not to spoil unification and by the conjugated fields).

Finally, the operator $\hat{\psi}_1\hat{\psi}_1\hat{\phi}\hat{h}\hat{Z}$ gives the wrong m_e/m_d ratio. The latter can be fixed if the first family left-handed or right-handed leptons mix. A mixing involving first family

[9] A term involving 2 brane fields and 1 bulk field is enhanced with respect to a term involving 1 brane field and 2 bulk fields (which is assumed to be $\mathcal{O}(1)$) by a factor $1/\lambda$, when expressed in terms of canonically normalized fields.

JHEP03(2009)031

left-handed leptons can also account for the solar angle and the other features of the neutrino mass matrix.

4.8 Summary of section 4

In this section, we embedded the PS model of section 2 into a supersymmetric 5D orbifold SO(10) model. In particular, the two discrete symmetries $\mathbf{Z}_2$ and R_P are embedded into a larger discrete group Z_{24} and into a continuous R-symmetry $\mathrm{U}(1)_R$ respectively. New fields are introduced in order to generate the proper vevs, to account for the neutrino sector and to preserve unification. We proceeded with an analysis of this setup as follows:

- We studied the possibility that the $\mathcal{O}(1)$ parameters and some of the mass scale hierarchies originate from a strong coupling regime through an order parameter $\lambda \approx 0.24$, in agreement with naive dimensional analysis.
- We wrote down the most general superpotential consistent with the symmetries, where we included two anomalously small coefficients, which represent, together with the strong coupling hierarchies, the seeds of all hierarchies of the model. In particular, the low-energy fermion mass hierarchies and small mixings have their very origin in this assumption.
- The mass scales of the model in section 2, M_R and M_L, and the compactification scale M_c turn out to be related to the cutoff scale $\Lambda \approx 10^{17}\,\mathrm{GeV}$ by powers of the order parameter λ up to $\mathcal{O}(1)$ coefficients. The field content at every scale is such that the MSSM unification of gauge couplings is preserved ("magic field sets"), but takes place at the higher scale Λ.
- In the neutrino sector we find good agreement with the data up to $\mathcal{O}(1)$ coefficients without making further assumptions. In particular, we obtain a large atmospheric mixing by means of an unusual mechanism.
- We studied gauge coupling unification in more detail to obtain a prediction for $\alpha_s(M_Z)$ and the (new) GUT scale Λ as a function of the small thresholds of the model. Depending on the $\mathcal{O}(1)$ uncertainties of such thresholds, we find that it is possible to obtain a prediction for $\alpha_s(M_Z)$ that improves on the standard MSSM prediction.
- We computed the proton lifetime resulting from our unified setup. The contribution to the decay rate from d=5 operators is strongly suppressed, which is a well-known consequence of the $\mathrm{U}(1)_R$ symmetry. The contribution from d=6 operators leads to a proton partial lifetime $1/\Gamma(p \to \pi^0 e^+) \sim 3 \times 10^{34}$ years, which is consistent with the present bound from SuperKamiokande and within the reach of future experiments.
- The further suppression of the first family charged fermion masses is also a consequence of the model. On the other hand, in order to account for the quantitative aspects of the spectrum associated to the first family, it may be necessary to introduce some type of flavour dynamics. We briefly sketched a possible implementation of this possibility.

JHEP03(2009)031

5 Conclusions

Following [1], we illustrated a neutrino-inspired supersymmetric model of fermion masses and mixings. As in the case of the second and third neutrinos in the context of the single right-handed dominance mechanism, the dominant exchange of a single set of left-handed messengers, with unconstrained, $\mathcal{O}(1)$ couplings accounts for most features of the masses and mixings of the second and third families and for the main qualitative features associated to the first family. While some specific flavour dynamics may need to be invoked for a quantitative description of the first family, it is impressive that so many other features do not actually need a flavour symmetry or other dynamics to be explained. Among them, we cite the suppression of the mass of the second family of charged fermions with respect to the third one, $|V_{cb}| \sim m_s/m_b$, $(m_\tau/m_b)_{\rm GUT} \approx 1$, $(m_\mu/m_s)_{\rm GUT} \approx 3$, the larger suppression in the up quark sector, $m_c/m_t \ll m_s/m_b$, the further suppression of the first charged fermion family mass.

In particular, we discussed the flavour phenomenology and the possibility to embed the model in a Grand Unified setting, preserving gauge coupling unification.

The interactions of the MSSM fields with the left-handed and right-handed flavour-messengers living at energies much higher than the electroweak scale leave their imprint on the sfermion soft masses through radiative effects, which induces FCNC and LFV effects at low energy. The peculiar feature of our model is that the Yukawa interactions of the flavour messengers with all the three light families are described by $\mathcal{O}(1)$ couplings, leading to sizable flavour-violating effects in the sfermion mass matrices. As the model targets especially the second and third families, we concentrated on the $\tau \to \mu\gamma$ decay. The present limit $\mathrm{BR}(\tau \to \mu\,\gamma) \lesssim 6.8 \cdot 10^{-8}$ only gives a weak constraint on the supersymmetry parameter space, while a Super B-Factory able to reach a sensitivity of 10^{-9} would test a large portion of it. The structure of the radiatively-induced contributions to the soft masses in the moderate $\tan\beta$ regime, $\tilde{m}^2_{ij} = m_0^2\delta_{ij} + \sigma c_{ij} m_0^2$, is particularly promising for detecting LFV at colliders. This structure gives rise to large mixing between the second and third family independent of how small σ is. By making σ small the branching ratio $\mathrm{BR}(\tau \to \mu\,\gamma)$ can be kept under control, but the LFV effects at colliders do not get suppressed, as long as $|\tilde{m}_2 - \tilde{m}_3|$ does not get too small, because the mixing angle remains large in the $\sigma \to 0$ limit.

The model can be embedded in a SO(10) supersymmetric GUT in 5 dimensions. As usual in 5D GUTs, the doublet-triplet splitting and the suppression of dimension five operators contribution to proton decay can be easily obtained in terms of orbifold boundary conditions and an R-symmetry. The three MSSM families are embedded into the spinorial representation of SO(10), so that the successful SO(10) predictions of the SM fermion gauge quantum numbers is maintained. We exhibited a full model accounting for the vevs used in the generation of the flavour structure, among the other things.

Two nice features of the model we are proposing are the possibility to relate the $\mathcal{O}(1)$ parameters to strong couplings and the fact that one of the small order parameters arises from the strong coupling assumption, in particular from the loop factor l_4 in 4 dimensions, $\lambda \equiv 1/l_4^{1/4} \approx 0.24$.

Gauge coupling unification is obtained in 5D in a novel way. At each scale up to the

JHEP03(2009)031

cutoff $\Lambda \sim 10^{17}$ GeV the field content has the "magic" property that it exactly preserves the MSSM 1-loop successful prediction for α_s, despite the field content does not constitute a full SU(5) representation [30]. On the other hand the unification scale, here identified with the cutoff Λ, gets larger, thus helping to avoid a too fast proton decay rate. This is also true in the energy range between the compactification scale and the cutoff, where the KK towers of states enter the running of gauge couplings. This is quite unusual. A generic feature of 5D GUT models is in fact the presence of threshold effects associated to the tower of KK excitations associated with bulk fields (sometimes useful to improve the gauge coupling unification prediction). The latter are associated to the very mechanism of GUT breaking by orbifold boundary conditions, which splits the GUT multiplets in the KK tower. In our case, such thresholds do not arise at the 1-loop level, because the GUT multiplets are split into two "magic" sets of fields preserving the MSSM gauge coupling unification.

As for proton decay, dimension-five operators are strongly suppressed due to a $U(1)_R$ symmetry, while d=6 operators are important because the mass of the extra gauge bosons is not too large. The lower limit on the proton lifetime gives a lower limit on the compactification scale $M_c \gtrsim 9.5 \times 10^{15}$ GeV, which is compatible with a larger unification scale of $\Lambda \sim 10^{17}$ GeV.

Some interesting features also arise in the neutrino sector. Previously [1], the large atmospheric angle and the $\Delta m^2_{12}/\Delta m^2_{23}$ suppression were obtained essentially through the single right-handed neutrino dominance mechanism, which in fact motivates the idea underlying this flavour model. Here, we consider another, more economical option in which the large atmospheric mixing arises through a different, unusual mechanism. In our model, which involves in the see-saw more than the usual 3 singlet neutrinos (9, in fact), the 22, 23, 32, 33 entries of the light neutrino mass matrix turn out to be proportional to four matrix elements of the inverse heavy singlet neutrino mass matrix. Such elements turn out to be of the same size and their determinant turns out to be suppressed because it is related to elements of the singlet neutrino mass matrix. The atmospheric squared mass difference is determined, up to an $\mathcal{O}(1)$ factor, to the scale at which the flavour messengers live, which in turn is given in terms of the unification scale by eq. (4.12). We then get a large atmospheric angle θ_{23}, the atmospheric squared mass difference Δm^2_{23} at the correct scale, and the suppression of the solar squared mass difference Δm^2_{12} (in the context of normal hierarchical neutrinos) and of the θ_{13} angle.

The origin of the peculiar pattern of SM fermion masses and mixings might be related to the breaking of a flavour symmetry, or to localization in extra dimensions, or it could be entangled to the structure of string theory. All in all, we find interesting that so many features of the fermion spectrum could instead just be due to the relative lightness (and structure) of a single family of flavour messengers, with "horizontal" flavour dynamics playing essentially no role.

Acknowledgments

We thank Marco Serone for many useful discussions and Pietro Slavich for helpful advice with `SusyBSG`. This work was supported by the European Network of Theoretical Astroparticle Physics ILIAS/N6 (contract RII3-CT-2004-506222).

JHEP03(2009)031

A Renormalization group equations

In this appendix we present the 1-loop Renormalization Group Equations (RGE) of the effective model in section 2 above and below the scale M_R.

RGEs above M_R. The relevant superpotential above M_R is given by:

$$W_{\rm PS} = \lambda_i f_i^c F h + \lambda_i^c f_i F^c h + \alpha_i \phi f_i \bar{F} + \alpha_i^c \phi f_i^c \bar{F}^c + a \bar{F}^c X_c F^c + \bar{\sigma}_c \bar{F}_c' \Phi F^c + \sigma_c \bar{F}^c \Phi F_c',$$

while the SUSY breaking potential reads

$$\begin{aligned} V_{\rm SSB} = & \left(m_f^2\right)_{ij} \tilde{f}_i^* \tilde{f}_j + \left(m_{f^c}^2\right)_{ij} \tilde{f}_i^{c^*} \tilde{f}_j^c + m_h^2 \tilde{h}^* \tilde{h} + m_\phi^2 \tilde{\phi}^* \tilde{\phi} + m_{\bar{F}}^2 \tilde{F}^* \tilde{F} + m_{\bar{\bar{F}}}^2 \tilde{\bar{F}}^* \tilde{\bar{F}} + m_{F^c}^2 \tilde{F^c}^* \tilde{F^c} \\ & + m_{\bar{F}^c}^2 \tilde{\bar{F}^c}^* \tilde{\bar{F}^c} + m_{\bar{F}_c'}^2 \tilde{\bar{F}_c'}^* \tilde{\bar{F}_c'} + m_{\bar{\bar{F}}_c'}^2 \tilde{\bar{\bar{F}}}_c'^* \tilde{\bar{\bar{F}}}_c' + m_\Phi^2 \tilde{\Phi}^* \tilde{\Phi} + m_X^2 \tilde{X}^* \tilde{X} + m_{X^c}^2 \tilde{X^c}^* \tilde{X^c} \\ & + m_H^2 \tilde{H}^* \tilde{H} + \Big(A_i^\lambda \tilde{f^c}_i \tilde{F} \tilde{h} + A_i^{\lambda^c} \tilde{f}_i \tilde{F^c} \tilde{h} + A_i^\alpha \tilde{\phi} \tilde{f}_i \tilde{\bar{F}} + A_i^{\alpha^c} \tilde{\phi} \tilde{f^c}_i \tilde{\bar{F}^c} + A^a \tilde{X^c} \tilde{\bar{F}^c} \tilde{F^c} \\ & + A^{\sigma_c} \tilde{\bar{F}^c} \tilde{\Phi} \tilde{F}_c' + A^{\bar{\sigma}_c} \tilde{\bar{F}}_c' \tilde{\Phi} \tilde{F^c} + \text{h.c.} \Big) + \frac{1}{2} \Big(M_4 \tilde{W}_4 \tilde{W}_4 + M_L \tilde{W}_L \tilde{W}_L + M_R \tilde{W}_R \tilde{W}_R + \text{h.c.} \Big). \end{aligned}$$

- Yukawa RGEs:

$$\begin{aligned} (4\pi)^2 \frac{d}{dt} \lambda_i &= \left(8|\vec{\lambda}|^2 + 4|\vec{\lambda^c}|^2 \right) \lambda_i + \frac{15}{8} \vec{\alpha^c} \cdot \vec{\lambda}\, \alpha_i^c - \left(\frac{15}{2} g_4^2 + 3 g_L^2 + 3 g_R^2 \right) \lambda_i \\ (4\pi)^2 \frac{d}{dt} \lambda_i^c &= \left(8|\vec{\lambda^c}|^2 + 4|\vec{\lambda}|^2 + \frac{15}{8} \bar{\sigma}_c^2 + \frac{3}{4} a^2 \right) \lambda_i^c + \frac{15}{8} \vec{\alpha} \cdot \vec{\lambda^c}\, \alpha_i - \left(\frac{15}{2} g_4^2 + 3 g_L^2 + 3 g_R^2 \right) \lambda_i^c \\ (4\pi)^2 \frac{d}{dt} \alpha_i &= \left(\frac{19}{4} |\vec{\alpha}|^2 + |\vec{\alpha^c}|^2 \right) \alpha_i + 2 \vec{\lambda^c} \cdot \vec{\alpha}\, \lambda_i^c - \left(\frac{31}{2} g_4^2 + 3 g_L^2 \right) \alpha_i \\ (4\pi)^2 \frac{d}{dt} \alpha_i &= \left(\frac{19}{4} |\vec{\alpha}|^2 + |\vec{\alpha^c}|^2 \right) \alpha_i + 2 \vec{\lambda^c} \cdot \vec{\alpha}\, \lambda_i^c - \left(\frac{31}{2} g_4^2 + 3 g_L^2 \right) \alpha_i \\ (4\pi)^2 \frac{d}{dt} \alpha_i^c &= \left(\frac{19}{4} |\vec{\alpha^c}|^2 + |\vec{\alpha}|^2 + \frac{15}{8} \sigma_c^2 + \frac{3}{4} a^2 \right) \alpha_i^c + 2 \vec{\lambda} \cdot \vec{\alpha^c}\, \lambda_i - \left(\frac{31}{2} g_4^2 + 3 g_R^2 \right) \alpha_i^c \\ (4\pi)^2 \frac{d}{dt} a &= \left(\frac{7}{2} a^2 + \frac{15}{8} \left(\sigma_c^2 + \bar{\sigma}_c^2 \right) + \frac{15}{8} |\vec{\alpha^c}|^2 + 2 |\vec{\lambda^c}|^2 \right) a - \left(\frac{15}{2} g_4^2 + 7 g_R^2 \right) a \\ (4\pi)^2 \frac{d}{dt} \sigma_c &= \left(\frac{19}{4} \sigma_c^2 + \bar{\sigma}_c^2 + \frac{15}{8} |\vec{\alpha^c}|^2 + \frac{3}{4} a^2 \right) \sigma_c - \left(\frac{31}{2} g_4^2 + 3 g_R^2 \right) \sigma_c \\ (4\pi)^2 \frac{d}{dt} \bar{\sigma}_c &= \left(\frac{19}{4} \bar{\sigma}_c^2 + \sigma_c^2 + 2 |\vec{\lambda^c}|^2 + \frac{3}{4} a^2 \right) \bar{\sigma}_c - \left(\frac{31}{2} g_4^2 + 3 g_R^2 \right) \bar{\sigma}_c \end{aligned}$$

- A-terms:

$$\begin{aligned} (4\pi)^2 \frac{d}{dt} A_i^\lambda = & \left(6|\vec{\lambda}|^2 + 4|\vec{\lambda^c}|^2 \right) A_i^\lambda + \left(18 \vec{\lambda} \cdot \vec{A^\lambda} \right) + 8 \vec{\lambda^c} \cdot \vec{A^{\lambda^c}} \lambda_i \\ & + \left(\frac{15}{8} \vec{\alpha^c} \cdot \vec{A^\lambda} + \frac{15}{4} \vec{\lambda} \cdot \vec{A^{\alpha^c}} \right) \alpha_i^c + \frac{15}{2} g_4^2 \left(2 M_4 \lambda_i - A_i^\lambda \right) \\ & + 3 g_L^2 \left(2 M_L \lambda_i - A_i^\lambda \right) + 3 g_R^2 \left(2 M_R \lambda_i - A_i^\lambda \right) \end{aligned}$$

JHEP03(2009)031

$$
\begin{aligned}
(4\pi)^2\frac{d}{dt}A_i^{\lambda^c} &= \left(6|\vec{\lambda^c}|^2+4|\vec{\lambda}|^2+\frac{15}{8}\bar{\sigma}_c^2+\frac{3}{4}a^2\right)A_i^{\lambda^c}\\
&+\left(18\vec{\lambda^c}\cdot\vec{A}^{\lambda^c}+8\vec{\lambda}\cdot\vec{A}^{\lambda}+\frac{15}{4}\bar{\sigma}_cA^{\bar{\sigma}_c}+\frac{3}{2}aA_a\right)\lambda_i^c\\
&+\left(\frac{15}{8}\vec{\alpha}\cdot\vec{A}^{\lambda^c}+\frac{15}{4}\vec{\lambda^c}\cdot\vec{A}^{\alpha}\right)\alpha_i\\
&+\frac{15}{2}g_4^2\left(2M_4\lambda_i^c-A_i^{\lambda^c}\right)+3g_L^2\left(2M_L\lambda_i^c-A_i^{\lambda^c}\right)\\
&+3g_R^2\left(2M_R\lambda_i^c-A_i^{\lambda^c}\right)\\
(4\pi)^2\frac{d}{dt}A_i^{\alpha} &= \left(\frac{23}{8}|\vec{\alpha}|^2+|\vec{\alpha^c}|^2\right)A_i^{\alpha}+\left(\frac{91}{8}\vec{\alpha}\cdot\vec{A}^{\alpha}+2\vec{\alpha^c}\cdot\vec{A}^{\alpha^c}\right)\alpha_i\\
&+\left(2\vec{\lambda^c}\cdot\vec{A}^{\alpha}+4\vec{\alpha}\cdot\vec{A}^{\lambda^c}\right)\lambda_i^c+\frac{31}{2}g_4^2\left(2M_4\alpha_i-A_i^{\alpha}\right)\\
&+3g_L^2\left(2M_L\alpha_i-A_i^{\alpha}\right)\\
(4\pi)^2\frac{d}{dt}A_i^{\alpha^c} &= \left(\frac{23}{8}|\vec{\alpha^c}|^2+|\vec{\alpha}|^2+\frac{15}{8}\sigma_c^2+\frac{3}{4}a^2\right)A_i^{\alpha^c}\\
&+\left(\frac{91}{8}\vec{\alpha^c}\cdot\vec{A}^{\alpha^c}+2\vec{\alpha}\cdot\vec{A}^{\alpha}+\frac{15}{4}\sigma_cA^{\sigma_c}+\frac{3}{2}aA_a\right)\alpha_i^c\\
&+\left(2\vec{\lambda}\cdot\vec{A}^{\alpha^c}+4\vec{\alpha^c}\cdot\vec{A}^{\lambda}\right)\lambda_i\\
&+\frac{31}{2}g_4^2\left(2M_4\alpha_i^c-A_i^{\alpha^c}\right)+3g_R^2\left(2M_R\alpha_i^c-A_i^{\alpha^c}\right)\\
(4\pi)^2\frac{d}{dt}A^{a} &= \left(\frac{21}{2}a^2+\frac{15}{8}(\sigma_c^2+\bar{\sigma}_c^2)+\frac{15}{8}|\vec{\alpha^c}|^2+2|\vec{\lambda^c}|^2\right)A^a\\
&+\left(\frac{15}{4}(\sigma_cA^{\sigma_c}+\bar{\sigma}_cA^{\bar{\sigma}_c})+\frac{15}{4}\vec{\alpha^c}\cdot\vec{A}^{\alpha^c}+4\vec{\lambda^c}\cdot\vec{A}^{\lambda^c}\right)a\\
&+\frac{15}{2}g_4^2\left(2M_4a-A^a\right)+7g_R^2\left(2M_Ra-A^a\right)\\
(4\pi)^2\frac{d}{dt}A^{\sigma_c} &= \left(\frac{57}{4}\sigma_c^2+\bar{\sigma}_c^2+\frac{15}{8}|\vec{\alpha^c}|^2+\frac{3}{4}a^2\right)A^{\sigma_c}\\
&+\left(2\bar{\sigma}_cA^{\bar{\sigma}_c}+\frac{15}{4}\vec{\alpha^c}\cdot\vec{A}^{\alpha^c}+\frac{3}{2}aA^a\right)\sigma_c\\
&+\frac{31}{2}g_4^2\left(2M_4\sigma_c-A^{\sigma_c}\right)+3g_R^2\left(2M_R\sigma_c-A^{\sigma_c}\right)\\
(4\pi)^2\frac{d}{dt}A^{\bar{\sigma}_c} &= \left(\frac{57}{4}\bar{\sigma}_c^2+\sigma_c^2+2|\vec{\lambda^c}|^2+\frac{3}{4}a^2\right)A^{\bar{\sigma}_c}\\
&+\left(2\sigma_cA^{\sigma_c}+4\vec{\lambda^c}\cdot\vec{A}^{\lambda^c}+\frac{3}{2}aA^a\right)\bar{\sigma}_c\\
&+\frac{31}{2}g_4^2\left(2M_4\bar{\sigma}_c-A^{\bar{\sigma}_c}\right)+3g_R^2\left(2M_R\bar{\sigma}_c-A^{\bar{\sigma}_c}\right)
\end{aligned}
$$

JHEP03(2009)031

- Soft masses:

$$
\begin{aligned}
(4\pi)^2\frac{d}{dt}\left(m_f^2\right)_{ij} &= \left(2\lambda_i^c\lambda_k^c+\frac{15}{8}\alpha_i\alpha_k\right)\left(m_f^2\right)_{kj}+\left(m_f^2\right)_{ik}\left(2\lambda_k^c\lambda_j^c+\frac{15}{8}\alpha_k\alpha_j\right)\\
&\quad+4\left(m_{F^c}^2+m_h^2\right)\lambda_i^c\lambda_j^c+\frac{15}{4}\left(m_{\bar{F}}^2+m_\phi^2\right)\alpha_i\alpha_j\\
&\quad+4A_i^{\lambda^c}A_j^{\lambda^c}+\frac{15}{4}A_i^{\alpha}A_j^{\alpha}-15g_4^2M_4^2-6g_L^2M_L^2\\
(4\pi)^2\frac{d}{dt}(m_{f^c}^2)_{ij} &= \left(2\lambda_i\lambda_k+\frac{15}{8}\alpha_i^c\alpha_k^c\right)(m_{f^c}^2)_{kj}+(m_{f^c}^2)_{ik}\left(2\lambda_k\lambda_j+\frac{15}{8}\alpha_k^c\alpha_j^c\right)\\
&\quad+4\left(m_F^2+m_h^2\right)\lambda_i\lambda_j+\frac{15}{4}\left(m_{\bar{F}^c}^2+m_\phi^2\right)\alpha_i^c\alpha_j^c\\
&\quad+4A_i^{\lambda}A_j^{\lambda}+\frac{15}{8}A_i^{\alpha^c}A_j^{\alpha^c}-15g_4^2M_4^2-6g_R^2M_R^2\\
(4\pi)^2\frac{d}{dt}m_h^2 &= 8\left(\left(|\vec{\lambda}|^2+|\vec{\lambda^c}|^2\right)m_h^2+\left(m_{f^c}^2\right)_{ij}\lambda_i\lambda_j+\left(m_f^2\right)_{ij}\lambda_i^c\lambda_j^c+m_F^2|\vec{\lambda}|^2\right.\\
&\quad\left.+m_{F^c}^2|\vec{\lambda^c}|^2+|\vec{A^\lambda}|^2+|\vec{A^{\lambda^c}}|^2\right)-6g_L^2M_L^2-6g_R^2M_R^2\\
(4\pi)^2\frac{d}{dt}m_\phi^2 &= \frac{15}{8}\left(\sum_i(\alpha_i^2+\alpha_i^{c2})m_\phi^2+(m_f^2)_{ij}\alpha_i\alpha_j+(m_{f^c}^2)_{ij}\alpha_i^c\alpha_j^c+m_{\bar{F}}^2|\vec{\alpha}|^2\right.\\
&\quad\left.+m_{\bar{F}^c}^2|\vec{\alpha^c}|^2+|\vec{A^\alpha}|^2+|\vec{A^{\alpha^c}}|^2\right)-32g_4^2M_4^2\\
(4\pi)^2\frac{d}{dt}m_F^2 &= 4\left(|\vec{\lambda}|^2m_F^2+(m_{f^c}^2)_{ij}\lambda_i\lambda_j+m_h^2|\vec{\lambda}|^2+|\vec{A^\lambda}|^2\right)-15g_4^2M_4^2-6g_L^2M_L^2\\
(4\pi)^2\frac{d}{dt}m_{\bar{F}}^2 &= \frac{15}{4}\left(|\vec{\alpha}|^2m_{\bar{F}}^2+(m_f^2)_{ij}\alpha_i\alpha_j+m_\phi^2|\vec{\alpha}|^2+|\vec{A^\alpha}|^2\right)-15g_4^2M_4^2-6g_L^2M_L^2\\
(4\pi)^2\frac{d}{dt}m_{F^c}^2 &= \left(4|\vec{\lambda^c}|^2+\frac{3}{2}a^2+\frac{15}{4}{\bar{\sigma_c}}^2\right)m_{F^c}^2+4(m_f^2)_{ij}\lambda_i^c\lambda_j^c+4m_h^2|\vec{\lambda^c}|^2\\
&\quad+\frac{3}{2}\left(m_{X^c}^2+m_{\bar{F}^c}^2\right)a^2+\frac{15}{4}\left(m_\Phi^2+m_{\bar{F}_c{}'}^2\right){\bar{\sigma_c}}^2+4|\vec{A^{\lambda^c}}|^2+\frac{3}{2}A^{a2}+\\
&\quad\frac{15}{4}A^{\bar{\sigma}_c2}-15g_4^2M_4^2-6g_R^2M_R^2\\
(4\pi)^2\frac{d}{dt}m_{\bar{F}_c}^2 &= \left(\frac{15}{4}|\vec{\alpha^c}|^2+\frac{3}{2}a^2+\frac{15}{4}\sigma_c^2\right)m_{\bar{F}^c}^2+\frac{15}{4}\left(m_{f^c}^2\right)_{ij}\alpha_i^c\alpha_j^c+\frac{15}{4}m_\phi^2|\vec{\alpha^c}|^2\\
&\quad+\frac{3}{2}\left(m_{X^c}^2+m_{F^c}^2\right)a^2+\frac{15}{4}\left(m_\Phi^2+m_{F_c'}^2\right){\bar{\sigma_c}}^2+\frac{15}{4}|\vec{A^{\alpha^c}}|^2+\frac{3}{2}A^{a2}\\
&\quad+\frac{15}{4}A^{\sigma^c2}-15g_4^2M_4^2-6g_R^2M_R^2\\
(4\pi)^2\frac{d}{dt}m_{F_c'}^2 &= \frac{15}{4}\left(\sigma_c^2m_{F_c'}^2+(m_\Phi^2+m_{\bar{F}_c}^2)\sigma_c^2+A^{\sigma_c2}\right)-15g_4^2M_4^2-6g_R^2M_R^2\\
(4\pi)^2\frac{d}{dt}m_{\bar{F}_c'}^2 &= \frac{15}{4}\left({\bar{\sigma_c}}^2m_{\bar{F}_c'}^2+(m_\Phi^2+m_{F^c}^2){\bar{\sigma_c}}^2+A^{\bar{\sigma}_c2}\right)-15g_4^2M_4^2-6g_R^2M_R^2\\
(4\pi)^2\frac{d}{dt}m_{X^c}^2 &= \frac{3}{2}\left(a^2m_{X^c}^2+(m_{F^c}^2+m_{\bar{F}^c}^2)a^2+A^{a2}\right)-16g_R^2M_R^2\\
(4\pi)^2\frac{d}{dt}m_\Phi^2 &= \frac{15}{8}\left(\left(\sigma_c^2+{\bar{\sigma_c}}^2\right)m_\Phi^2+\left(m_{\bar{F}^c}^2+m_{F_c'}^2\right)\sigma_c^2+\left(m_{F^c}^2+m_{\bar{F}_c{}'}^2\right){\bar{\sigma_c}}^2\right.\\
&\quad\left.+A^{\sigma_c2}+A^{\bar{\sigma}_c2}\right)-32g_4^2M_4^2
\end{aligned}
$$

RGEs between M_L and M_R. Neglecting interactions with singlet neutrinos lighter than M_R, the superpotential between M_L and M_R is given by:

$$W = \left(\alpha_q^A\right)_i q_i \bar{Q} A_\phi + \left(\alpha_l^A\right)_i l_i \bar{L} A_\phi + \left(\alpha_q^T\right)_i q_i \bar{L} \bar{T}_\phi + \left(\alpha_l^T\right)_i l_i \bar{Q} T_\phi + \left(\alpha_q^G\right)_i G_\phi q_i \bar{Q} + \lambda_i^u u_i^c Q h_u + \lambda_i^d d_i^c Q h_d + \lambda_i^e e_i^c L h_d. \tag{A.1}$$

The boundary conditions for the above Yukawas at M_R read:

$$\lambda^u = \lambda^d = \lambda^e = \lambda$$
$$\sqrt{24}\,\alpha_q^A = -\frac{\sqrt{24}}{3}\alpha_l^A = \sqrt{2}\,\alpha_q^T = \sqrt{2}\,\alpha_l^T = \alpha_q^G = \alpha.$$

The first and the second line of eq. (A.1) are decoupled: in particular the RGEs for the second line Yukawas and soft masses are MSSM-like.

References

[1] L. Ferretti, S.F. King and A. Romanino, *Flavour from accidental symmetries*, *JHEP* **11** (2006) 078 [hep-ph/0609047] [SPIRES].

[2] S.M. Barr, *An* SO*(10) Model Of Fermion Masses*, *Phys. Rev.* **D 24** (1981) 1895 [SPIRES]; *A simple and predictive model for quark and lepton masses*, *Phys. Rev. Lett.* **64** (1990) 353 [SPIRES]; *A predictive hierarchical mode of quark and lepton masses*, *Phys. Rev.* **D 42** (1990) 3150 [SPIRES];
B.A. Dobrescu and E.H. Simmons, *Top-bottom splitting in technicolor with composite scalars*, *Phys. Rev.* **D 59** (1999) 015014 [hep-ph/9807469] [SPIRES];
S.M. Barr, *Flavor without flavor symmetry*, *Phys. Rev.* **D 65** (2002) 096012 [hep-ph/0106241] [SPIRES].

[3] S.F. King, *Atmospheric and solar neutrinos with a heavy singlet*, *Phys. Lett.* **B 439** (1998) 350 [hep-ph/9806440] [SPIRES]; *Atmospheric and solar neutrinos from single right-handed neutrino dominance and* U(1) *family symmetry*, *Nucl. Phys.* **B 562** (1999) 57 [hep-ph/9904210] [SPIRES]; *Large mixing angle MSW and atmospheric neutrinos from single right-handed neutrino dominance and* U(1) *family symmetry*, *Nucl. Phys.* **B 576** (2000) 85 [hep-ph/9912492] [SPIRES]; *Constructing the large mixing angle MNS matrix in see-saw models with right-handed neutrino dominance*, *JHEP* **09** (2002) 011 [hep-ph/0204360] [SPIRES].

[4] L.J. Hall, R. Rattazzi and U. Sarid, *The top quark mass in supersymmetric* SO(10) *unification*, *Phys. Rev.* **D 50** (1994) 7048 [hep-ph/9306309] [SPIRES];
P. Ciafaloni, A. Romanino and A. Strumia, *Lepton flavor violations in* SO(10) *with large* $\tan\beta$, *Nucl. Phys.* **B 458** (1996) 3 [hep-ph/9507379] [SPIRES].

[5] M. Drees, *Intermediate scale symmetry breaking and the spectrum of super partners in superstring inspired supergravity models*, *Phys. Lett.* **B 181** (1986) 279 [SPIRES];
J.S. Hagelin and S. Kelley, *Sparticle masses ad a probe of gut physics*, *Nucl. Phys.* **B 342** (1990) 95 [SPIRES].

[6] M. Dine and A.E. Nelson, *Dynamical supersymmetry breaking at low-energies*, *Phys. Rev.* **D 48** (1993) 1277 [hep-ph/9303230] [SPIRES];
M. Dine, A.E. Nelson and Y. Shirman, *Low-energy dynamical supersymmetry breaking simplified*, *Phys. Rev.* **D 51** (1995) 1362 [hep-ph/9408384] [SPIRES];

JHEP03(2009)031

M. Dine, A.E. Nelson, Y. Nir and Y. Shirman, *New tools for low-energy dynamical supersymmetry breaking*, *Phys. Rev.* **D 53** (1996) 2658 [hep-ph/9507378] [SPIRES];
G.F. Giudice and R. Rattazzi, *Theories with gauge-mediated supersymmetry breaking*, *Phys. Rept.* **322** (1999) 419 [hep-ph/9801271] [SPIRES].

[7] D.E. Kaplan, G.D. Kribs and M. Schmaltz, *Supersymmetry breaking through transparent extra dimensions*, *Phys. Rev.* **D 62** (2000) 035010 [hep-ph/9911293] [SPIRES];
Z. Chacko, M.A. Luty, A.E. Nelson and E. Ponton, *Gaugino mediated supersymmetry breaking*, *JHEP* **01** (2000) 003 [hep-ph/9911323] [SPIRES].

[8] F. Borzumati and A. Masiero, *Large muon and electron number violations in supergravity theories*, *Phys. Rev. Lett.* **57** (1986) 961 [SPIRES].

[9] R. Barbieri and L.J. Hall, *Signals for supersymmetric unification*, *Phys. Lett.* **B 338** (1994) 212 [hep-ph/9408406] [SPIRES];
R. Barbieri, L.J. Hall and A. Strumia, *Violations of lepton flavor and CP in supersymmetric unified theories*, *Nucl. Phys.* **B 445** (1995) 219 [hep-ph/9501334] [SPIRES].

[10] J. Hisano, T. Moroi, K. Tobe and M. Yamaguchi, *Lepton-flavor violation via right-handed neutrino Yukawa couplings in supersymmetric standard model*, *Phys. Rev.* **D 53** (1996) 2442 [hep-ph/9510309] [SPIRES].

[11] T. Moroi, *The muon anomalous magnetic dipole moment in the minimal supersymmetric standard model*, *Phys. Rev.* **D 53** (1996) 6565 [*Erratum ibid* **D 56** (1997) 4424] [hep-ph/9512396] [SPIRES].

[12] G. Isidori and A. Retico, $B_{s,d} \to \ell^+\ell^-$ *and* $K_L \to \ell^+\ell^-$ *in SUSY models with non-minimal sources of flavour mixing*, *JHEP* **09** (2002) 063 [hep-ph/0208159] [SPIRES];
G. Isidori and P. Paradisi, *Hints of large* $\tan\beta$ *in flavour physics*, *Phys. Lett.* **B 639** (2006) 499 [hep-ph/0605012] [SPIRES].

[13] G. Degrassi, P. Gambino and P. Slavich, *SusyBSG: a fortran code for* $BR[B \to X_s\gamma]$ *in the MSSM with Minimal Flavor Violation*, *Comput. Phys. Commun.* **179** (2008) 759 [arXiv:0712.3265] [SPIRES].

[14] MEGA collaboration, M.L. Brooks et. al., *New limit for the family-number non-conserving decay* $\mu^+ \to e^+_\gamma$, *Phys. Rev. Lett.* **83** (1999) 1521 [hep-ex/9905013] [SPIRES].

[15] BABAR collaboration, B. Aubert et. al., *Search for lepton flavor violation in the decay* $\tau^\pm \to \mu^\pm\gamma$, *Phys. Rev. Lett.* **95** (2005) 041802 [hep-ex/0502032] [SPIRES].

[16] BABAR collaboration, B. Aubert et. al., *Search for lepton flavor violation in the decay* $\tau^\pm \to e^\pm\gamma$, *Phys. Rev. Lett.* **96** (2006) 041801 [hep-ex/0508012] [SPIRES].

[17] Heavy Flavor Averaging Group (HFAG) collaboration, E. Barberio et. al., *Averages of b-hadron properties at the end of 2006*, arXiv:0704.3575 [SPIRES].

[18] CDF collaboration, T. Aaltonen et. al., *Search for* $B_s \to \mu^+\mu^-$ *and* $B_d \to \mu^+\mu^-$ *decays with* $2fb^{-1}$ *of* $p\bar{p}$ *collisions*, *Phys. Rev. Lett.* **100** (2008) 101802 [arXiv:0712.1708] [SPIRES].

[19] CDF collaboration, A. Abulencia et. al., *Observation of* $B^0_s - \bar{B}^0_s$ *oscillations*, *Phys. Rev. Lett.* **97** (2006) 242003 [hep-ex/0609040] [SPIRES].

[20] M. Passera, W.J. Marciano and A. Sirlin, *The muon g-2 and the bounds on the Higgs boson mass*, *Phys. Rev.* **D 78** (2008) 013009 [arXiv:0804.1142] [SPIRES].

[21] M. Bona et. al., *SuperB: a high-luminosity asymmetric* e^+e^- *super flavor factory. Conceptual design report*, arXiv:0709.0451 [SPIRES].

JHEP03(2009)031

[22] WMAP collaboration, D.N. Spergel et. al., *Wilkinson Microwave Anisotropy Probe (WMAP) Three Year results: Implications for cosmology*, *Astrophys. J. Suppl.* **170** (2007) 377 [astro-ph/0603449] [SPIRES].

[23] J.R. Ellis, T. Falk and K.A. Olive, *Neutralino-stau coannihilation and the cosmological upper limit on the mass of the lightest supersymmetric particle*, *Phys. Lett.* **B 444** (1998) 367 [hep-ph/9810360] [SPIRES];
J.R. Ellis, T. Falk, K.A. Olive and M. Srednicki, *Calculations of neutralino stau coannihilation channels and the cosmologically relevant region of MSSM parameter space*, *Astropart. Phys.* **13** (2000) 181 [*Erratum ibid* **15** (2001) 413] [hep-ph/9905481] [SPIRES].

[24] M. Drees and M.M. Nojiri, *The neutralino relic density in minimal $N = 1$ supergravity*, *Phys. Rev.* **D 47** (1993) 376 [hep-ph/9207234] [SPIRES].

[25] G. Bélanger, F. Boudjema, A. Pukhov and A. Semenov, *MicrOMEGAs2.0: A program to calculate the relic density of dark matter in a generic model*, *Comput. Phys. Commun.* **176** (2007) 367 [hep-ph/0607059] [SPIRES]; *Dark matter direct detection rate in a generic model with MicrOMEGAs2.1*, arXiv:0803.2360 [SPIRES].

[26] N. Arkani-Hamed, H.-C. Cheng, J.L. Feng and L.J. Hall, *Probing lepton flavor violation at future colliders*, *Phys. Rev. Lett.* **77** (1996) 1937 [hep-ph/9603431] [SPIRES].

[27] L.J. Hall and Y. Nomura, *Gauge unification in higher dimensions*, *Phys. Rev.* **D 64** (2001) 055003 [hep-ph/0103125] [SPIRES].

[28] G. Altarelli and F. Feruglio, SU(5) *grand unification in extra dimensions and proton decay*, *Phys. Lett.* **B 511** (2001) 257 [hep-ph/0102301] [SPIRES];
A. Hebecker and J. March-Russell, *A minimal $S^1/(Z_2 \times Z_2')$ orbifold GUT*, *Nucl.Phys.* **B 613** (2001) 3 [hep-ph/0106166] [SPIRES].

[29] R. Dermisek and A. Mafi, SO(10) *grand unification in five dimensions: proton decay and the mu problem*, *Phys. Rev.* **D 65** (2002) 055002 [hep-ph/0108139] [SPIRES];
H.D. Kim and S. Raby, *Unification in* $5D$ SO(10), *JHEP* **01** (2003) 056 [hep-ph/0212348] [SPIRES];
M.L. Alciati, F. Feruglio, Y. Lin and A. Varagnolo, *Fermion masses and proton decay in a minimal five- dimensional* SO(10) *model*, *JHEP* **11** (2006) 039 [hep-ph/0603086] [SPIRES].

[30] L. Calibbi, L. Ferretti, A. Romanino and R. Ziegler, *Gauge coupling unification, the GUT scale and magic fields*, *Phys. Lett.***B 672** (2009) 152 [arXiv:0812.0342] [SPIRES].

[31] Z. Chacko, M.A. Luty and E. Ponton, *Massive higher-dimensional gauge fields as messengers of supersymmetry breaking*, *JHEP* **07** (2000) 036 [hep-ph/9909248] [SPIRES].

[32] L.J. Hall and Y. Nomura, *A complete theory of grand unification in five dimensions*, *Phys. Rev.* **D 66** (2002) 075004 [hep-ph/0205067][SPIRES].

[33] L.J. Hall, J. March-Russell, T. Okui and D. Tucker-Smith, *Towards a theory of flavor from orbifold GUTs*, *JHEP* **09** (2004) 026 [hep-ph/0108161] [SPIRES];
M.L. Alciati, F. Feruglio, Y. Lin and A. Varagnolo, *Fermion masses and proton decay in a minimal five- dimensional* SO(10) *model*, *JHEP* **11** (2006) 039 [hep-ph/0603086] [SPIRES].

[34] N. Sakai and T. Yanagida, *Proton decay in a class of supersymmetric grand unified models*, *Nucl. Phys.* **B 197** (1982) 533 [SPIRES].

[35] A. Hebecker and J. March-Russell, *Proton decay signatures of orbifold GUTs*, *Phys. Lett.* **B 539** (2002) 119 [hep-ph/0204037] [SPIRES].

JHEP03(2009)031

[36] J. Hisano, H. Murayama and T. Yanagida, *Nucleon decay in the minimal supersymmetric* SU(5) *grand unification*, *Nucl. Phys.***B 402** (1993) 46 [hep-ph/9207279] [SPIRES];
J. Hisano, *Proton decay in the supersymmetric grand unified models*, hep-ph/0004266 [SPIRES].

[37] Super-Kamiokande collaboration, M. Shiozawa et. al., *Search for proton decay via* $p \to e^+\pi^0$ *in a large water cherenkov detector*, *Phys. Rev. Lett.* **81** (1998) 3319 [hep-ex/9806014] [SPIRES].

[38] M. Shiozawa, *Study of 1-Megaton water cherenkov detectors for the future proton decay search*, *AIP Conf. Proc.* **533** (2000) 21 [SPIRES].

JHEP03(2009)031